



Chinese Pharmaceutical Association
Institute of Materia Medica, Chinese Academy of Medical Sciences

Acta Pharmaceutica Sinica B

www.elsevier.com/locate/apsb
www.sciencedirect.com



ORIGINAL ARTICLE

Endothelial METRNL determines circulating METRNL level and maintains endothelial function against atherosclerosis



Sili Zheng^{a,†}, Zhiyong Li^{a,†}, Jie Song^{a,†}, Pin Wang^{a,†}, Jian Xu^{b,†},
Wenjun Hu^a, Yi Shi^c, Qi Qi^a, Zhuwei Miao^a, Yunfeng Guan^a,
Chaoyu Miao^{a,*}

^aDepartment of Pharmacology, Second Military Medical University/Naval Medical University, Shanghai 200433, China

^bChanghai Hospital, Second Military Medical University/Naval Medical University, Shanghai 200433, China

^cZhongshan Hospital, Fudan University, Shanghai 200032, China

Received 14 August 2022; received in revised form 11 November 2022; accepted 18 November 2022

KEY WORDS

METRNL;
Secreted protein;
Endothelium;
Endothelial function;
Bone marrow;
Atherosclerosis

Abstract METRNL is a recently identified secreted protein with emerging functions. This study is to find major cellular source of circulating METRNL and to determine METRNL novel function. Here, we show METRNL is abundant in human and mouse vascular endothelium and released by endothelial cells using endoplasmic reticulum-Golgi apparatus pathway. By creating endothelial cell-specific *Metrnl* knockout mice, combined with bone marrow transplantation to produce bone marrow-specific deletion of *Metrnl*, we demonstrate that most of circulating METRNL (approximately 75%) originates from the endothelial cells. Both endothelial and circulating METRNL decrease in atherosclerosis mice and patients. By generating endothelial cell-specific *Metrnl* knockout in apolipoprotein E-deficient mice, combined with bone marrow-specific deletion of *Metrnl* in apolipoprotein E-deficient mice, we further demonstrate that endothelial METRNL deficiency accelerates atherosclerosis. Mechanically, endothelial METRNL deficiency causes vascular endothelial dysfunction including vasodilation impairment *via* reducing eNOS phosphorylation at Ser1177 and inflammation activation *via* enhancing NFκB pathway, which promotes the susceptibility of atherosclerosis. Exogenous METRNL rescues METRNL deficiency induced endothelial dysfunction. These findings reveal that METRNL is a new endothelial substance not only determining the circulating METRNL level but also regulating endothelial function for vascular health and disease. METRNL is a therapeutic target against endothelial dysfunction and atherosclerosis.

*Corresponding author. Tel.: +86 21 81871271; fax: +86 21 65493951.

E-mail address: cymiao@smmu.edu.cn (Chaoyu Miao).

[†]These authors made equal contributions to this work.

Peer review under the responsibility of Chinese Pharmaceutical Association and Institute of Materia Medica, Chinese Academy of Medical Sciences.

<https://doi.org/10.1016/j.apsb.2022.12.008>

2211-3835 © 2023 Chinese Pharmaceutical Association and Institute of Materia Medica, Chinese Academy of Medical Sciences. Production and hosting by Elsevier B.V. This is an open access article under the CC BY-NC-ND license (<http://creativecommons.org/licenses/by-nc-nd/4.0/>).

© 2023 Chinese Pharmaceutical Association and Institute of Materia Medica, Chinese Academy of Medical Sciences. Production and hosting by Elsevier B.V. This is an open access article under the CC BY-NC-ND license (<http://creativecommons.org/licenses/by-nc-nd/4.0/>).

1. Introduction

Secreted proteins play critical roles in physiological and pathological processes and can be used as biomarkers and therapies for aging and disease^{1–3}. METRNL has been identified as a novel secreted protein by us and others^{4–6}. We also named it Subfatin, because of its beneficial adipokine nature and the highest presence in subcutaneous fat among different fat tissues^{4,5}. Bioinformatic analysis predicts that the METRNL proteins encoded in the mouse, rat, and human genomes contain 311 amino acids, with a NH₂-terminal signal peptide of 45 amino acids, suggesting a mature secreted protein containing 266 amino acids^{4–6}. METRNL secretion has been verified in HEK293 cells, COS-7 cells, HEK293F cells, 3T3-L1 adipocytes, primary adipocytes, adipose tissue, and gut tissue^{4–7}.

The physiological contribution of METRNL is emerging³. This protein plays a role in neurite outgrowth, insulin sensitization, white adipose browning, and immunoinflammatory response. In neurocytes, METRNL protein promotes neurite outgrowth and neuroblast migration, implying an effect on the neuronal differentiation and nervous tissue development⁶. In adipose tissue, adipocyte-specific overexpression of *Metrnl* in transgenic mice antagonizes high fat diet (HFD)-induced insulin resistance by enhancing adipocyte differentiation and attenuating inflammation⁵, while an abrupt increase of METRNL by administration of *Metrnl*-expressing adenoviral vectors or METRNL protein transiently induces white adipose browning within less than ten days⁸. In addition, treatment with METRNL protein attenuates HFD-induced insulin resistance in skeletal muscle of mice⁹. In immunoinflammatory response, METRNL regulates the expression of cytokines, and affects the susceptibility of mice to endotoxin-induced sepsis^{10,11} and dextran sodium sulfate-induced ulcerative colitis¹², suggesting it has an anti-inflammatory effect. Research concerning this novel bioactive protein has been initiated, and its functional spectrum in health and disease and its mechanism(s) of action remain largely unknown.

Circulating METRNL is reduced in patients with newly diagnosed type 2 diabetes mellitus¹³ and coronary artery disease¹⁴. However, it is still unknown which cells secrete the protein into the circulation, since our earlier experiments failed to show a significant reduction in circulating METRNL level by specific knockout of the protein in white adipocytes or intestinal epithelial cells, although we demonstrated a rich presence of METRNL in these cells^{5,7}.

The present study aimed to identify the major cellular source of circulating METRNL and to unravel the role played by the protein in these cells. Using cell-specific gene knockout and double gene knockout strategies, combined with bone marrow (BM) transplantation to produce BM-specific interventions, we demonstrate that METRNL is a new endothelial bioactive protein. Vascular endothelial cells are the major cellular source for circulating METRNL. Deletion of endothelial *Metrnl* causes endothelial dysfunction and accelerates atherosclerosis, indicating endothelial METRNL plays a critical role in maintaining vascular

health. METRNL is a therapeutic target against endothelial dysfunction and atherosclerosis.

2. Methods

2.1. Mouse models

Animal experiments were performed in accordance with the National Institute of Health Guide for the Care and Use of Laboratory Animals, and approved by the Institutional Animal Care and Use Committee of the Second Military Medical University. *Tek-Cre* mice [*B6. Cg-Tg(Tek-cre)12Flv/J*] were purchased from the Jackson Laboratory (Bar Harbor, ME, USA). C57BL/6 mice, CD45.1 mice, and apolipoprotein E-deficient (*ApoE*^{−/−}) mice were purchased from the Shanghai Research Center for Model Organisms (Shanghai, China). *Metrnl* floxed (*Metrnl*^{loxP/loxP}) mice have been characterized in our previous study⁵, and in the present experiments, these mice were used to generate endothelial cell-specific *Metrnl* knockout mice (*Metrnl*^{loxP/loxP}*Tek-Cre*, EC-*Metrnl*^{−/−}) by crossing *Metrnl*^{loxP/loxP} mice with *Tek-Cre* mice (Supporting Information Fig. S1). Littermates were used as controls in all experiments. EC-*Metrnl*^{−/−} mouse model was then bred into the *ApoE*^{−/−} genetic background to generate double gene knockout mice (*ApoE*^{−/−}EC-*Metrnl*^{−/−}) (Supporting Information Fig. S2). Atherosclerosis was induced by HFD for 10 or 22 weeks in *ApoE*^{−/−} and *ApoE*^{−/−}EC-*Metrnl*^{−/−} mice, or spontaneously occurred at one year of age under normal chow in these mice. HFD contained 42.5% fat, 1.3% cholesterol, and 0.3% cholate (Shanghai Slac Laboratory Animal Co., Ltd., Shanghai, China). Myocardial infarction in mice was produced according to our previous study¹⁵ (Supporting Information, Methods). All mice were housed on a 12-h light-dark cycle with free access to food and water. Animals were anaesthetized with one intraperitoneal injection of pentobarbital sodium (100 mg/kg) (Sigma–Aldrich, St. Louis, MO, USA) before experiments, with the level of anaesthesia being verified by pinching.

2.2. BM transplantation

BM transplantation experiments were performed as described previously¹⁶. Six-week-old male C57BL/6 mice (recipients) were exposed to 8.5 Gy irradiation using a ⁶⁰Co source to destroy their own BM 2.5 h before transplantation of BM cells from donors. Donor BM cells were extracted from donor mice (EC-*Metrnl*^{−/−} mice or wild type littermates, or CD45.1 mice) by flushing femur and tibia bones with phosphate-buffered saline (PBS). Each recipient mouse was injected with 1 × 10⁷ BM cells (in 200 μL PBS) through tail vein, and was given antibiotics in drinking water with 100 mg/L levofloxacin and 200 mg/L metronidazole in the following two weeks. Seven weeks after BM transplantation, the recipient mice who received BM from EC-*Metrnl*^{−/−} mice or wild type littermates were euthanized by one intraperitoneal injection of pentobarbital sodium (100 mg/kg), with venous blood collected for METRNL measurement and BM cells obtained for transplantation efficacy identification

based on polymerase chain reaction (PCR) analysis. Transplantation efficacy analysis by flow cytometry in BM cells and blood mononuclear cells was also performed in other recipient mice who received BM from CD45.1 mice. BM transplantation in atherosclerosis study was also performed (Supporting Information, Methods).

2.3. Human plasma collection

A total of 32 patients from the out-patient units of the Changhai Hospital, Second Military Medical University, Shanghai, China, between December 26, 2015 and January 21, 2016 were enrolled, including 21 patients with myocardial infarction (MI) and 11 non-MI age- and gender-matched controls. MI was diagnosed by the cardiologists. MI patients received angiography examination, indicating they had coronary atherosclerosis. In the group of MI patients with atherosclerosis, 17 males and four females with 40–89 years of age (mean age 64.7 years), and in the control group, eight males and three females with 42–79 years of age (mean age 62.5 years) were included (Supporting Information Table S1). Venous blood samples were collected for plasma cardiac troponin I and METRNL assays. The study was conducted in compliance with the Declaration of Helsinki and was approved by the medical ethical committee of the Changhai Hospital. Written consent was obtained from all participants.

2.4. Vascular reactivity analysis

Vascular contractions and relaxations were measured in isolated aortic rings, as described in our previous studies^{17,18}. Briefly, the descending thoracic aorta was removed and cut into 3 mm wide rings which were suspended in organ chambers filled with Krebs-Henseleit solution (NaCl 118.4 mmol/L, KCl 4.7 mmol/L, CaCl₂ 2.5 mmol/L, MgSO₄ 1.2 mmol/L, KH₂PO₄ 1.2 mmol/L, NaHCO₃ 25.0 mmol/L, glucose 11.1 mmol/L and CaNa₂-EDTA 0.026 mmol/L), aerated with 95% O₂ and 5% CO₂. Vascular reactivity was measured as changes in isometric tension using IT1-25 transducers and an IOX computerized system (EMKA Technologies, Paris, France). Each aortic ring was allowed to equilibrate during 60 min at a resting tension of 1.5 g. After several stimulations with KCl (60 mmol/L), and re-equilibration, a single dose of phenylephrine (Phe, 3×10^{-7} mol/L; Sigma–Aldrich) was used to induce vascular contraction. When the Phe-induced contraction reached a plateau, the endothelium-dependent vasodilator acetylcholine (ACh, a muscarinic agonist; Sigma–Aldrich) was added in a cumulative manner to obtain concentration–relaxation curves. After re-equilibration and obtaining a second Phe-induced contraction, the endothelium-independent vasodilator sodium nitroprusside (SNP, an exogenous NO-donor; Sigma–Aldrich) was added in a cumulative manner. The relaxation was expressed as percent of the pre-contraction to Phe. Another set of experiments was performed to know whether or not exogenous METRNL could affect aortic response when added to the organ bath. Recombinant mouse METRNL protein (300 ng/mL, R&D Systems, Minneapolis, MN, USA) was added 20 min before the first Phe-induced contraction.

2.5. Atherosclerotic lesion analysis

Atherosclerotic lesions were analyzed as described in our previous study¹⁷. Briefly, the heart was fully exposed, and blood was collected by inferior vena cava puncture for serum lipids assay.

After perfusion, the heart and the entire aorta from the junction with the heart to the iliac bifurcation were collected for careful removal of perivascular adipose tissue, and then immersed in freshly prepared 4% paraformaldehyde during 24 h. The aorta was then processed for oil red O (ORO; Sigma–Aldrich) staining, while the heart was embedded in Jung Tissue freezing Medium (Leica Microsystems) for obtaining serial frozen sections of 8 μ m thickness. Hematoxylin–Eosin (Beyotime Biotechnology, Nantong, China) and ORO staining of the aortic root cross-sections were carried out. Lesion area analysis was performed (Supporting Information, Methods).

2.6. Cell culture, virus-mediated overexpression and knockdown of METRNL, immunohistochemistry, immunofluorescence, real time PCR, Western blotting, enzyme-linked immunosorbent assay (ELISA) measurements of METRNL, blood lipids assay, and ORO staining for lipid-laden macrophage

Described in our previous studies^{4,5,7,13,15,17–19} and in detail in the Supporting Information online (Methods).

2.7. Statistical analysis

All data are expressed as the mean \pm standard deviation error (SEM). Statistical analysis was performed with SPSS statistical software v25.0 (IBM corp, Chicago, IL, USA). All data were tested for normality by using the Kolmogorov–Smirnov test. If normality was confirmed and there were no significant differences in variance between groups (F test), the differences were evaluated by two-tailed Student's *t*-test; otherwise, the nonparametric Mann–Whitney U test was used. For the vascular reactivity studies, two-way analysis of variance (ANOVA) for repeated measures was used to compare two curves. *P*-values less than 0.05 were considered to indicate statistically significant differences.

3. Results

3.1. METRNL is highly present in vascular endothelium and secreted via a classical endoplasmic reticulum–Golgi apparatus pathway

To uncover the major source of circulating METRNL, our previous samples (human multi-organ tissue microarray, human tissue obtained during surgical interventions, or mouse tissue from normal animals)^{4,5,7} were re-examined, searching for the specific location of METRNL presence. Among 22 different human and murine tissues, the highest presence of METRNL, in both humans and mice, was observed in white adipose and gastrointestinal tissues (Supporting Information Table S1), in accordance with previous data^{4,5,7} demonstrating the protein mainly in white adipocytes and gastrointestinal epithelium. Unexpectedly, METRNL was abundant in human cerebral blood vessel (Fig. 1A), although its presence in human brain parenchyma was still low, as reported for mouse brain tissue^{4–8}. Furthermore, the high presence of METRNL was not limited to cerebral blood vessels, but was also evident in the vasculature of other tissues, in particular in fat depots (Fig. 1A).

Consistent with these results, *Metrl* was highly expressed in the murine aorta among different tissues, as detected by real time PCR (Fig. 1B). To further clarify the location of METRNL in the vascular wall, immunofluorescence was performed to detect the

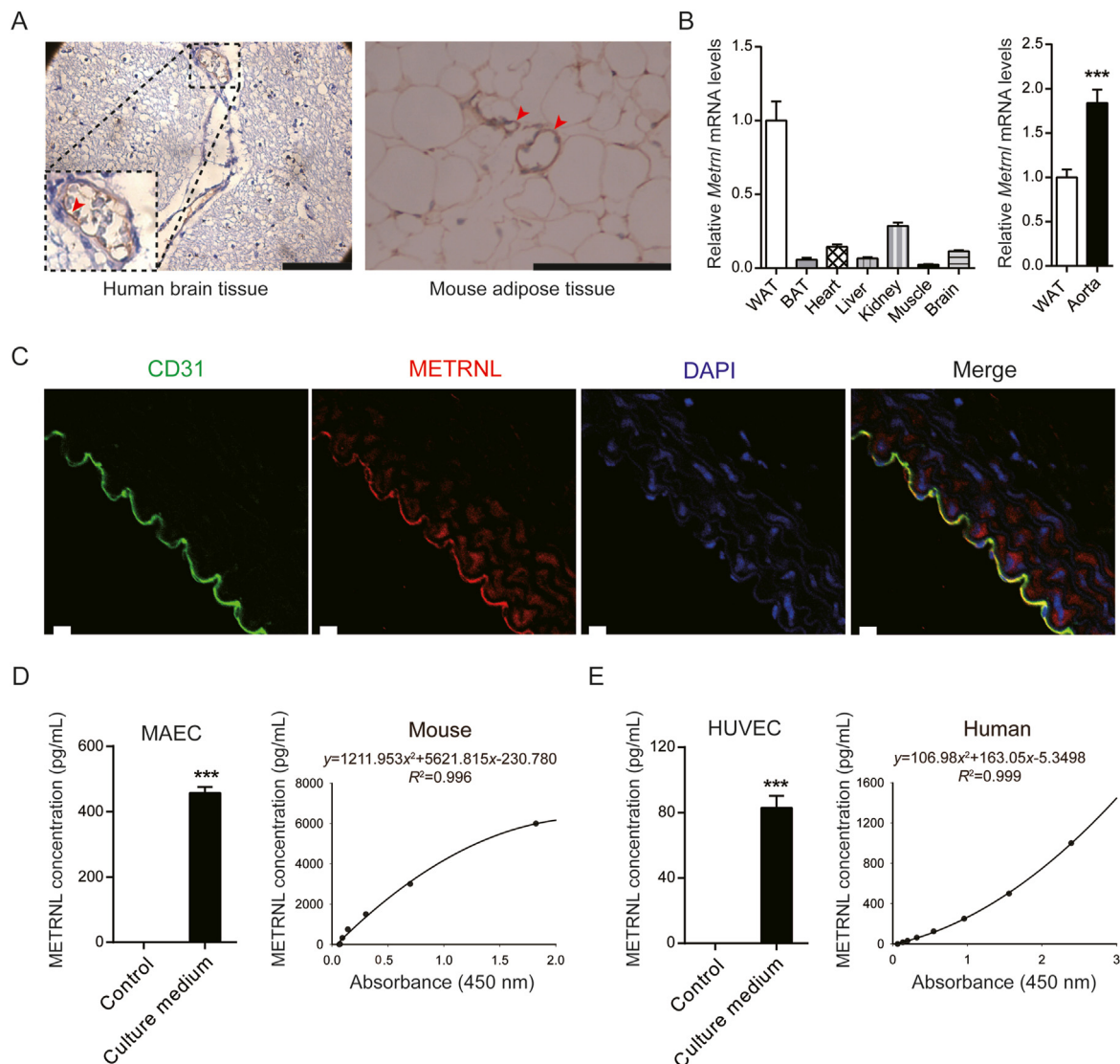


Figure 1 METRNL is highly present in the endothelium and secreted by endothelial cells. (A) METRNL in human and mouse blood vessels, indicated by arrows. Scale bar: 200 μ m. (B) *Metrn* mRNA in different mouse tissues ($n = 5-8$). WAT, white adipose tissue; BAT, brown adipose tissue. (C) METRNL and CD31 co-localized in mouse aortic endothelium. DAPI labels nuclei. Scale bar: 20 μ m. Five independent experiments performed. (D) METRNL secretion from primary cultured mouse aortic endothelial cells (MAECs) in serum-free culture medium during 12 h (left, $n = 3$) and representative enzyme-linked immunosorbent assay (ELISA) standard curve for measuring mouse METRNL concentrations in cell culture medium or blood serum/plasma (right). (E) METRNL secretion from primary cultured human umbilical vein endothelial cells (HUVECs) in serum-free culture medium during 3 h (left, $n = 6$) and representative ELISA standard curve for measuring human METRNL concentrations in cell culture medium or blood serum/plasma (right). Data are mean \pm SEM. *** $P < 0.001$ by two-tailed Student's t test in (B, D and E).

presence of the protein as well as that of cluster of differentiation (CD) 31 (a marker of endothelial cells) in mouse aortae. The results showed that METRNL and CD31 co-localized (Fig. 1C), indicating that the former is dominantly present in the endothelium.

To know whether or not endothelial cells release METRNL protein, primary cultured murine endothelial cells^{15,20} (Supporting Information Fig. S3) and human endothelial cells²¹ were used. Like in the culture medium of adipocytes or adipose tissue^{4,5}, METRNL was also detected in the medium bathing cultured mouse aortic endothelial cells (MAECs) (Fig. 1D), demonstrating that endothelial METRNL can be released. Such release of

METRNL was further observed in the culture medium of primary human umbilical vein endothelial cells (HUVECs) (Fig. 1E).

Further, the METRNL secretion pathway was studied. In HUVECs, *METRNL* gene overexpression mediated by adeno-associated virus (AAV) and knockdown mediated by lentivirus significantly increased and decreased the METRNL levels respectively, in both the cell and culture medium (Fig. 2A and B). The full-length METRNL protein encoded in the genome contains 311 amino acids, with a NH₂-terminal signal peptide (SP) of 45 amino acids⁴⁻⁶ (Fig. 2A). An AAV mediated overexpression of *METRNL* without SP domain (*METRNL*- Δ SP, Fig. 2C) was designed and transfected into HUVECs to

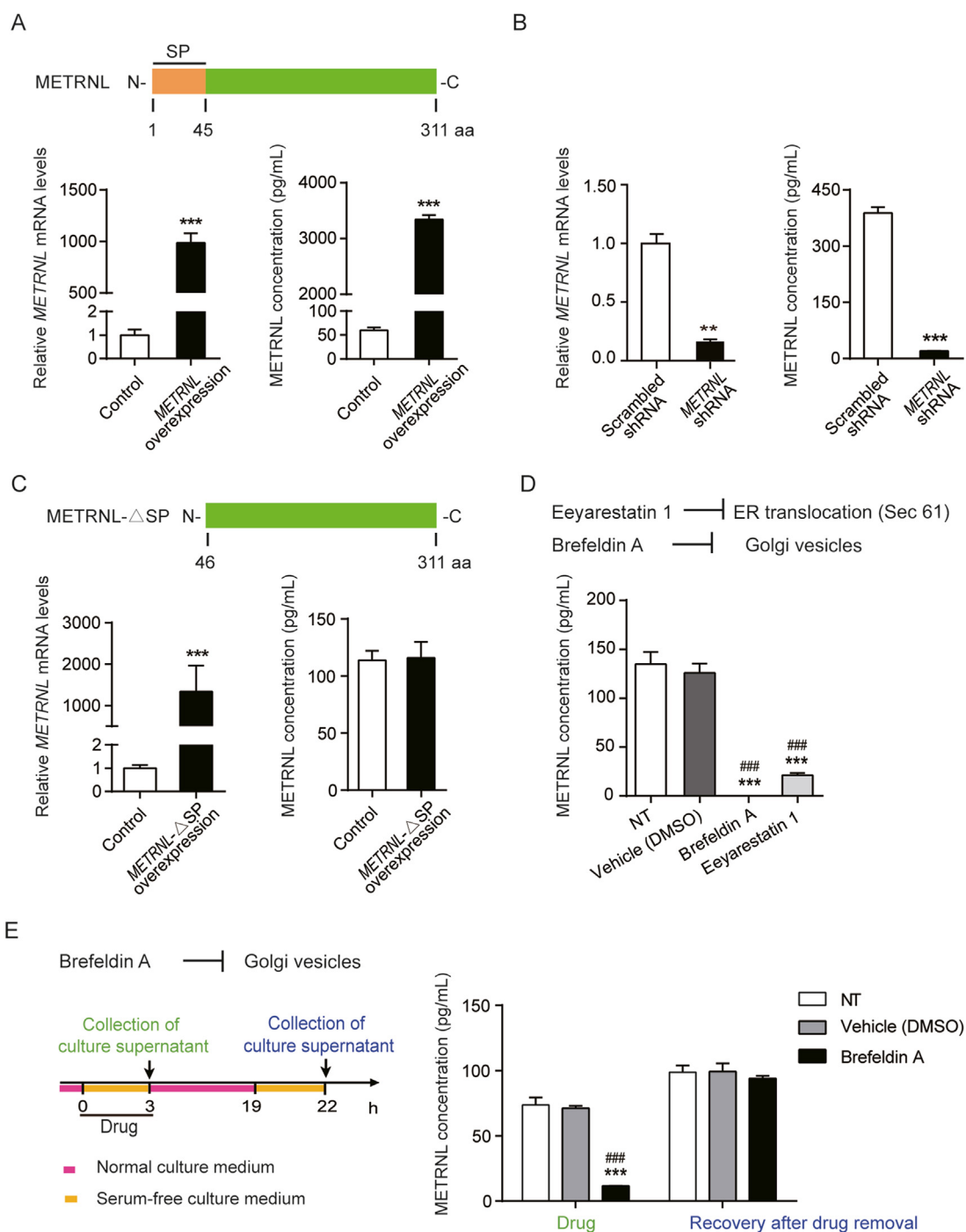


Figure 2 METRNL secretion by endothelial cells involves the classical ER–Golgi pathway. (A) Domain structure of human METRNL with the N-terminal signal peptide (SP) (up). METRNL mRNA expression (left) in HUVECs with adeno-associated virus (AAV)-mediated METRNL overexpression and METRNL concentrations (right) in the serum-free culture medium during 24 h ($n = 4–6$). (B) METRNL mRNA expression (left) in HUVECs with lentivirus-mediated METRNL knockdown and METRNL concentrations (right) in the serum-free culture medium during 24 h ($n = 4–6$). (C) Domain structure of human METRNL without SP region (METRNL-ΔSP, up). METRNL mRNA expression (left) in HUVECs with AAV-mediated overexpression of METRNL without SP domain and METRNL concentrations (right) in the serum-free culture medium during 24 h ($n = 3–4$). (D) METRNL secretion from primary cultured HUVECs inhibited by both eeyarestatin 1 (5 μg/mL) and brefeldin A (5 μg/mL) ($n = 3$). NT, no treatment as blank control. (E) Recovery of METRNL release from HUVECs after brefeldin A removal. Brefeldin A (5 μg/mL) or a solvent control (DMSO) was added to the serum-free culture medium 3 h before medium collection for METRNL measurement. Then the cells were washed for three times and incubated in normal culture medium without drugs for 16 h followed by another 3 h of serum-free medium incubation and METRNL detection of the culture supernatant ($n = 3$). NT, no treatment as blank control. Data are mean ± SEM. $**P < 0.01$, $***P < 0.001$ by two-tailed Student's t test in (A, B and C). $***P < 0.001$ vs. Vehicle; $###P < 0.001$ vs. NT by one-way ANOVA followed by Dunnett's t test in (D and E).

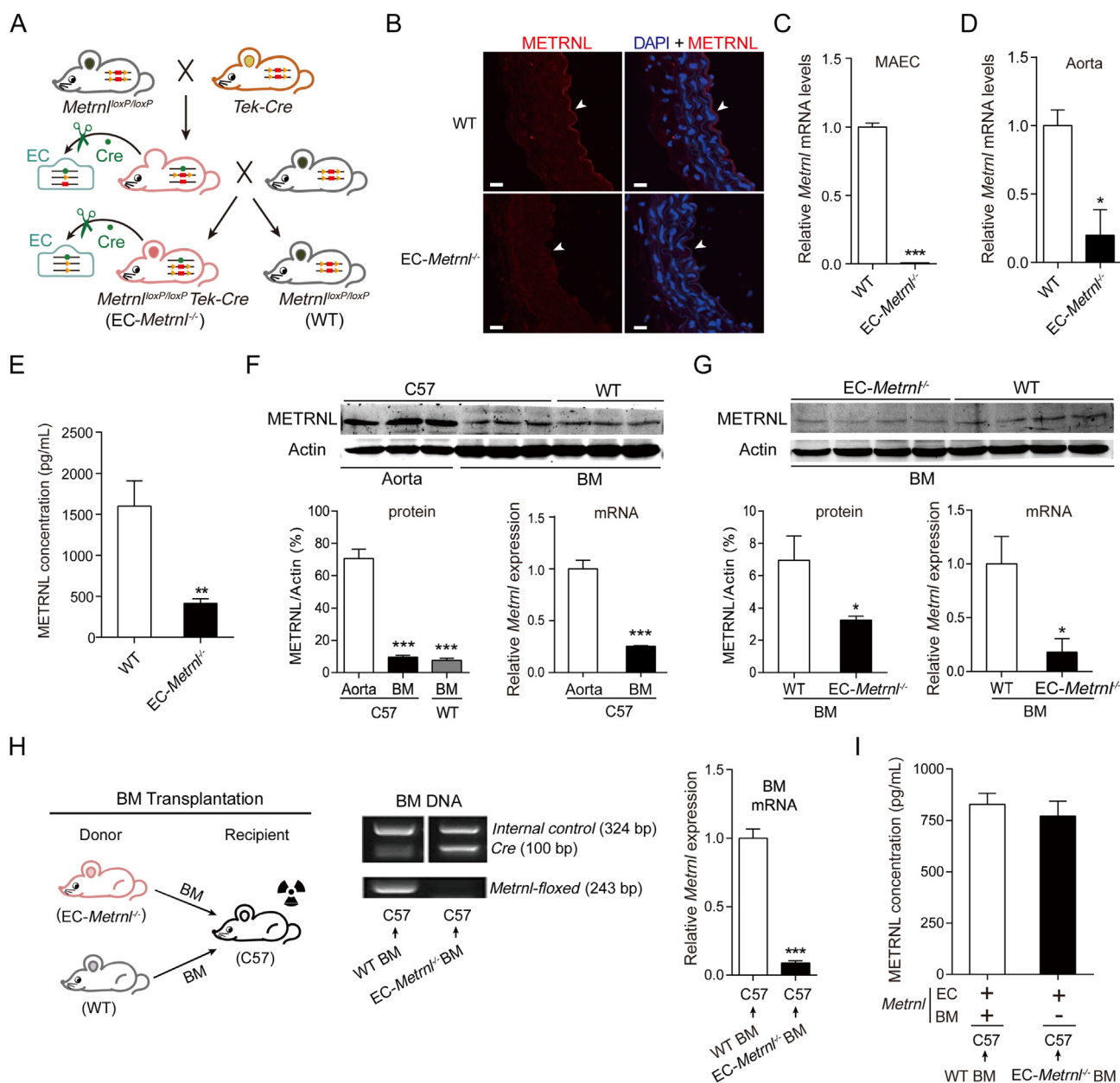


Figure 3 Endothelial METRNL deficiency reduces the circulating METRNL level. (A) Endothelial cell (EC)-specific *Metrn* knockout (*EC-Metrnl*^{-/-}) mice are generated by mating *Metrn*^{loxP/loxP} and *Tek-Cre* mice. (B) METRNL in the endothelium of aortae from *EC-Metrnl*^{-/-} and wild-type (WT) mice. Scale bar: 20 μ m. Four independent experiments performed. (C) *Metrn* mRNA levels in mouse aortic endothelial cells (MAECs) ($n = 6$). (D) *Metrn* mRNA levels in aortae with endothelium intact ($n = 3-4$). (E) Serum METRNL levels in *EC-Metrnl*^{-/-} and WT mice ($n = 16-17$). (F) Protein and mRNA levels of METRNL in aortae and bone marrow (BM) of C57BL/6 and WT mice ($n = 3-6$). (G) Protein and mRNA levels of METRNL in BM of *EC-Metrnl*^{-/-} and WT mice ($n = 4-7$). (H) Design of BM transplantation experiments (left), genotyping of BM DNA (middle), and *Metrn* mRNA expression in BM of chimeric C57BL/6 mice receiving donor BM cells from *EC-Metrnl*^{-/-} or WT mice (right) ($n = 11-12$). The recipient C57BL/6 mice using irradiation to destroy their own BM and then receiving donor BM cells from *EC-Metrnl*^{-/-} or WT mice. (I) Serum METRNL levels in chimeric C57BL/6 mice receiving donor BM cells from *EC-Metrnl*^{-/-} or WT mice ($n = 11$). +: normal expression of *Metrn*; -: deficient expression of *Metrn*. Data are mean \pm SEM. * $P < 0.05$, ** $P < 0.01$, *** $P < 0.001$ by two-tailed Student's *t* test in (C, E, F right, G, and H) and Mann-Whitney U test in (D). *** $P < 0.001$ vs. C57 Aorta by one-way ANOVA followed by Dunnett's *t* test in (F left).

determine whether the SP domain affects the release of METRNL; as expected, overexpression of *METRNL* without SP domain only increased the *METRNL* mRNA level inside the cell by more than 1000-fold, but did not increase the METRNL

protein level in the culture medium (Fig. 2C), suggesting that the SP region is required for the release of METRNL. This SP-guided secretion of protein is a characteristic for the classical endoplasmic reticulum (ER)-Golgi apparatus secretion

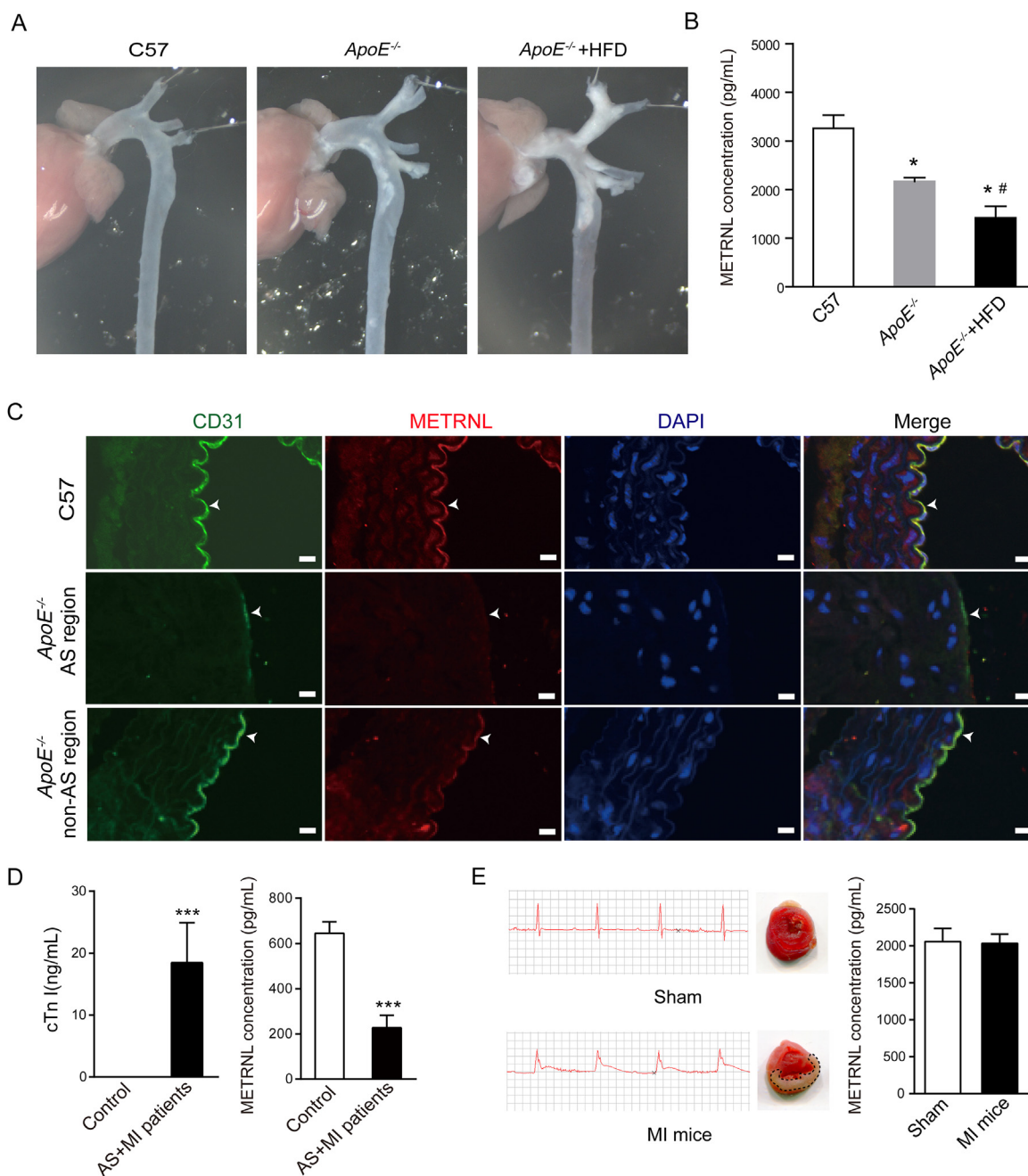


Figure 4 METRNL levels decrease in mice and humans with atherosclerosis. (A, B) Different extents of atherosclerosis are produced in one-year-old $ApoE^{-/-}$ mice, with more severe atherosclerosis in $ApoE^{-/-}$ mice fed high fat diet (HFD, for 22 weeks) than normal chow (A). Serum METRNL levels are reduced in $ApoE^{-/-}$ mice, with more reduction in $ApoE^{-/-}$ mice fed HFD than normal chow (B). $n = 4-5$. (C) METRNL and CD31 in the endothelium of aortae from normal control and $ApoE^{-/-}$ mice. Endothelial METRNL decreases in $ApoE^{-/-}$ mice, with obvious lack of endothelial METRNL in the region of atherosclerotic lesion (AS). Bar = 20 μm . Three independent experiments performed. (D) Plasma levels of cardiac troponin I (cTn I) and METRNL in control ($n = 11$) and myocardial infarction (MI) patients with atherosclerosis (AS) ($n = 21$). (E) Serum METRNL levels in mice 24 h after myocardial infarction (MI) produced by coronary artery ligation surgery (right). $n = 10$. Two independent experiments performed. Electrocardiograms of mice immediately after the surgery (left), and 2,3,5-triphenyltetrazolium chloride-stained heart sections 24 h after the surgery (middle) are shown. Sham: sham operation. Data are mean \pm SEM. * $P < 0.05$, # $P < 0.05$, *** $P < 0.001$ by two-tailed Student's t test in (D) and one-way ANOVA followed by two-tailed Student's t test in (B). * $P < 0.05$ vs. C57; # $P < 0.05$ vs. $ApoE^{-/-}$.

pathway. To further demonstrate that METRNL can be released by the classical secretion pathway, chemical inhibitors were used. The Sec61 channel is the translocon on the ER membrane that translocates the nascent polypeptide chain into the ER

lumen^{22,23}. Eeyarestatin 1 inhibits Sec61 hampering the construction of transport channels in ER membranes^{24,25}. Brefeldin A prevents the proper function of the Golgi apparatus by interrupting the transport of proteins from ER to it^{24,26}. Both

eeyarestatin 1 and brefeldin A markedly inhibited the release of METRNL from HUVECs (Fig. 2D and E), with no obvious changes in cell number and morphology during 3 h of treatment (Supporting Information Fig. S4), and METRNL release from endothelial cells totally recovered after removal of the brefeldin A (Fig. 2E), similar to the previous study showing that the inhibition by brefeldin A is reversible²⁷. The immunofluorescence co-localization of METRNL with calnexin (a marker of ER) or 58K (a marker of Golgi apparatus) also provided the evidence for the presence of METRNL in these organelles (Supporting Information Fig. S5). Thus, the present results indicate that METRNL secretion by endothelial cells involves the classical ER–Golgi pathway.

3.2. Endothelial METRNL deficiency reduces the circulating METRNL levels

To determine whether or not endothelial METRNL contributes to the circulating level of the protein, mice with endothelial cell-specific knockout of *Metrl* (EC-*Metrl*^{-/-}) were generated by mating *Metrl*^{loxP/loxP} with *Tek-Cre* mice (Fig. 3A and Fig. S1). *Metrl*^{loxP/loxP} mice were created in our previous study⁵. *Tek-Cre* mice, in which the expression of Cre recombinase is driven by a promoter of endothelial-specific *Tek* (also called *Tie2*)²⁸, were used to specifically delete endothelial *Metrl* by crossing with *Metrl*^{loxP/loxP} mice. The deficiency of METRNL in the endothelium was confirmed with immunofluorescence (Fig. 3B and Supporting Information Fig. S6). Real time PCR measurements showed that the gene expression of *Metrl* in isolated aortic endothelial cells was decreased by more than 95% in EC-*Metrl*^{-/-} compared with wild type mice (Fig. 3C). Similarly, in aortae with endothelium intact, the expression of *Metrl* was markedly reduced in EC-*Metrl*^{-/-} group (Fig. 3D). However, in aortae with endothelium removal, *Metrl* expression was comparable between EC-*Metrl*^{-/-} and wild type groups (Supporting Information Fig. S7A). We also detected *Metrl* mRNA levels in other tissues including white adipose tissue, liver, kidney and heart, showing no significant differences between EC-*Metrl*^{-/-} and wild type groups (Fig. S7B). These findings demonstrate a successful specific knockout of *Metrl* in the endothelium.

No visible phenotypic differences were observed between EC-*Metrl*^{-/-} and wild type mice. The genotypic ratio also fitted the Mendelian expectation. Moreover, both body weight and organ weights were within control values in EC-*Metrl*^{-/-} mice (Fig. S7C and S7D). Importantly, the serum levels of METRNL were reduced significantly in EC-*Metrl*^{-/-} mice, with an average reduction of 75% (Fig. 3E). Thus, the present results demonstrate that endothelial METRNL is a major contributor to the circulating levels of the protein.

3.3. Bone marrow does not contribute to the circulating METRNL levels

It has been recently reported that the recombinase Cre under control of the *Tek* promoter is also expressed in BM hematopoietic cells during development²⁹. To know the possible Cre mediated deletion of *Metrl* in BM cells that potentially contributes to the reduction of the circulating levels of the protein in EC-*Metrl*^{-/-} mice, METRNL expression was checked in BM

compared with aorta. Both protein and mRNA expression of METRNL in BM were much lower than in aorta (Fig. 3F). However, BM METRNL expression was indeed reduced in EC-*Metrl*^{-/-} mice compared with wild type mice, indicating that *Tek-Cre* mediates partial deletion of METRNL in BM of EC-*Metrl*^{-/-} mice (Fig. 3G). To determine whether or not the deficiency of BM METRNL contributes to the reduced circulating level of the protein in EC-*Metrl*^{-/-} mice, we performed BM transplantation experiments to produce BM-specific intervention model¹⁶. The recipient C57 mice (Fig. 3H) were irradiated to destroy their own BM, then they received BM transplantation from donors, EC-*Metrl*^{-/-} or wild type mice. After 7 weeks, transplantation efficacy was checked by BM DNA genotyping and *Metrl* expression (Fig. 3H) as well as by flow cytometry to determine BM cell replacement (Supporting Information Fig. S8). Serum METRNL levels were detected in chimeric C57 mice receiving donor BM cells from EC-*Metrl*^{-/-} or wild type mice. The results showed that the efficient *Metrl* deletion in BM of the C57 mice by successful replacement of BM cells (Fig. 3H and Fig. S8) did not affect the circulating METRNL levels (Fig. 3I), indicating that the reduced circulating METRNL level in EC-*Metrl*^{-/-} mice is due to METRNL deficiency in endothelial cells rather than in BM hematopoietic cells. These data suggest that the potential contribution due to *Metrl* knockout in hematopoietic cells to the reduced circulating METRNL levels is almost negligible.

3.4. Both endothelial and circulating METRNL decrease in atherosclerosis mice and humans

To examine the possible involvement of METRNL protein in disease states, circulating METRNL levels and aortic METRNL presence were determined in *ApoE*^{-/-} mice, an accepted animal model of atherosclerosis. One-year-old mice were used for detection. To obtain different extents of atherosclerosis, one group of *ApoE*^{-/-} mice was fed HFD during 22 weeks, the other mice were fed normal chow. Atherosclerosis occurred in multiple sites of the aortae and carotid arteries from *ApoE*^{-/-} mice, more severe in all *ApoE*^{-/-} mice fed HFD than normal chow (Fig. 4A and Supporting Information Fig. S9A). Serum METRNL levels were significantly reduced in *ApoE*^{-/-} mice compared with wild type mice, with more reduction in *ApoE*^{-/-} mice fed HFD (Fig. 4B). The presence of the METRNL protein was also reduced in the endothelium of aortae from *ApoE*^{-/-} mice, compared to those from wild type mice, with an obvious lack of endothelial METRNL in regions with atherosclerotic lesions (Fig. 4C and Supporting Information Fig. S10).

Further, a small samples of patients with myocardial infarction and coronary atherosclerosis were included for detection of circulating METRNL. The plasma cardiac troponin I levels were significantly increased in patients with myocardial infarction and atherosclerosis (Fig. 4D and Table S1), while their plasma METRNL levels were reduced significantly (Fig. 4D). To know whether myocardial infarction contributes to the reduction of circulating METRNL levels, serum METRNL levels were examined in animal model of myocardial infarction without atherosclerosis. The result showed that myocardial infarction did not induce any change of serum METRNL levels at 4 and 24 h after ligation of coronary artery in mice (Fig. 4E and Supporting

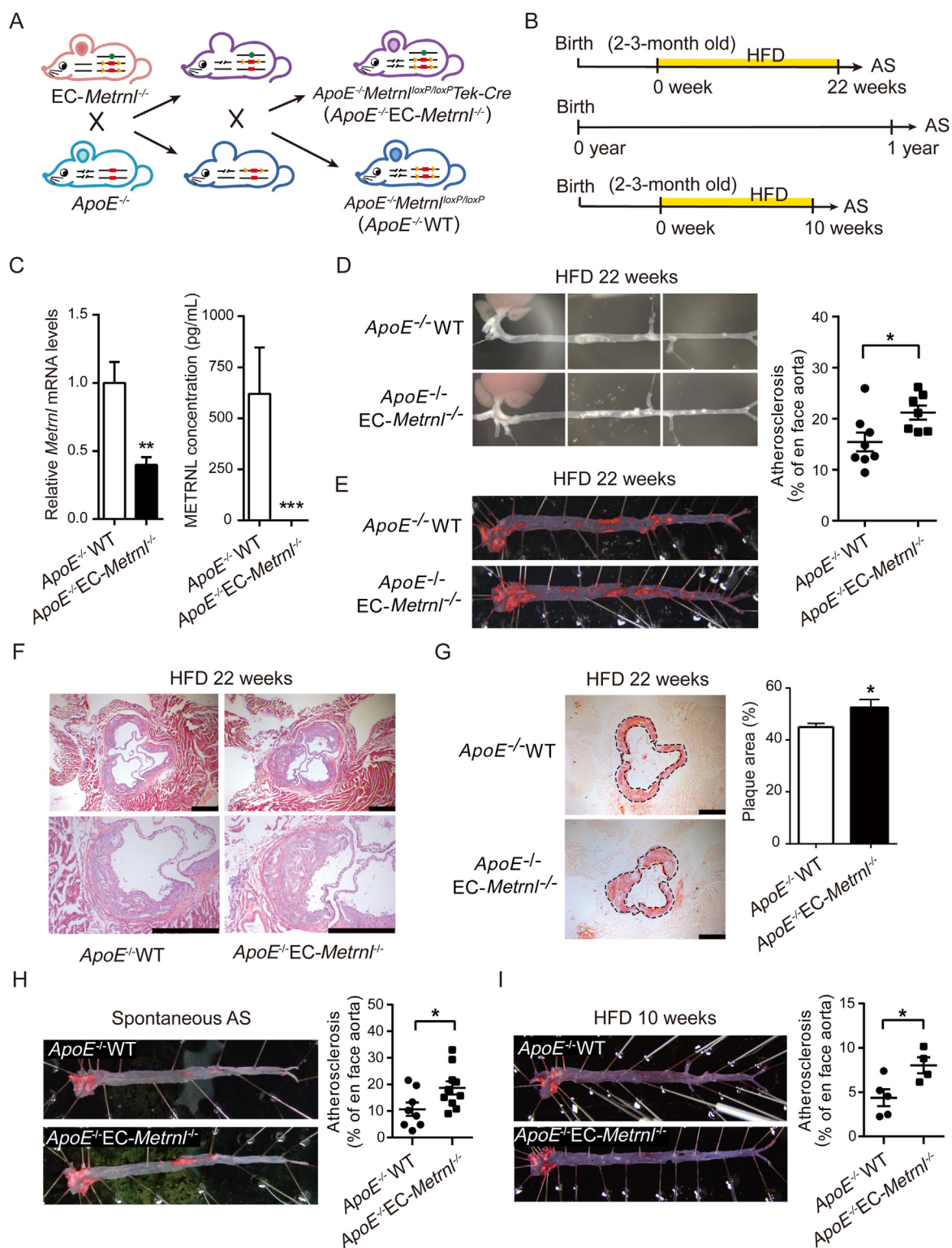


Figure 5 Endothelial METRNL deficiency accelerates atherosclerosis. (A) Double knockout mice with whole-body ApoE deficiency and endothelial cell-specific Metnrl deficiency (*ApoE^{-/-}EC-Metnrl^{-/-}*). (B) Experimental design of atherosclerosis studies in *ApoE^{-/-}EC-Metnrl^{-/-}* mice. Induction of atherosclerosis (AS) by HFD during long period (22 weeks) or relatively short period (10 weeks) starting from the age of two to three months, or observation of spontaneous atherosclerosis at the age of one year with normal chow diet. (C) Aortic *Metnrl* expression (left, $n = 7$) and serum METRNL levels (right, $n = 3-4$) in *ApoE^{-/-}EC-Metnrl^{-/-}* mice and *ApoE^{-/-}WT* littermates. (D) Atherosclerotic lesions in aortae from *ApoE^{-/-}EC-Metnrl^{-/-}* mice and *ApoE^{-/-}WT* littermates fed HFD for 22 weeks. (E) Oil red O (ORO) staining of aortae from *ApoE^{-/-}EC-Metnrl^{-/-}* mice and *ApoE^{-/-}WT* littermates fed HFD for 22 weeks ($n = 7-8$). (F and G) Hematoxylin and eosin staining (F) and ORO staining (G) of aortic roots ($n = 6-8$). Bar = 500 μ m. (H) Spontaneous atherosclerosis (AS) in aortae from one-year-old *ApoE^{-/-}EC-Metnrl^{-/-}* mice and *ApoE^{-/-}WT* littermates fed normal chow diet ($n = 8-10$). (I) Atherosclerotic lesions in aortae from *ApoE^{-/-}EC-Metnrl^{-/-}* mice and *ApoE^{-/-}WT* littermates fed HFD for 10 weeks ($n = 4-5$). Data are mean \pm SEM. * $P < 0.05$, ** $P < 0.01$ by two-tailed Student's *t* test in (C, E, G-I).

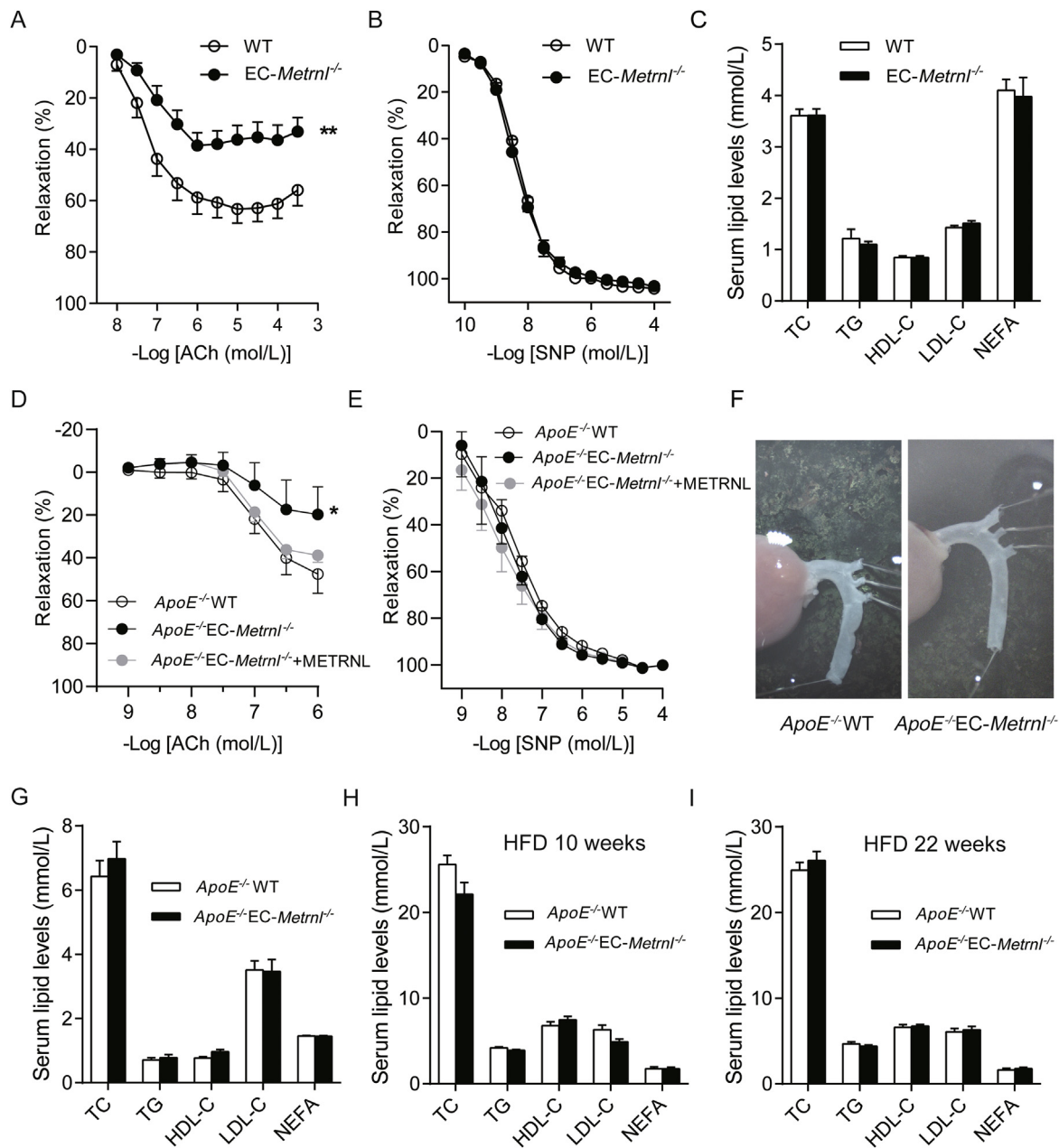


Figure 6 Endothelial METRNL deficiency impairs endothelium-dependent vascular relaxation with unchanged blood lipid levels. (A–C) Concentration–relaxation curves to acetylcholine (ACh, A) and sodium nitroprusside (SNP, B) in aortae ($n = 7–8$) from EC-Metrnl^{-/-} and WT mice with unchanged serum lipid levels (C, $n = 9–10$). (D–F) Concentration–relaxation curves to ACh (D) and SNP (E) in aortae ($n = 5$) from ApoE^{-/-}EC-Metrnl^{-/-} and ApoE^{-/-}WT mice at 3 months of age under normal chow without atherosclerosis in aortae (F). (G–I) Serum lipid levels in ApoE^{-/-}EC-Metrnl^{-/-} mice and ApoE^{-/-}WT littermates without atherosclerosis at 3 months of age under normal chow (G), with mild atherosclerosis after 10 weeks of HFD (H) and with severe atherosclerosis after 22 weeks of HFD (I). HDL-C, high density lipoprotein-cholesterol; LDL-C, low density lipoprotein-cholesterol; TG, triglycerides; TC, total cholesterol; NEFA, nonesterified fatty acids. Data are mean \pm SEM. * $P < 0.05$, ** $P < 0.01$ by two-way ANOVA in (A and D).

Information Fig. S9B and S9C). Thus, a significant reduction of circulating METRNL levels in patients with myocardial infarction and atherosclerosis seems due to atherosclerosis rather than myocardial infarction. These observations suggest a clinical cardiovascular implication for METRNL in atherosclerosis.

3.5. Endothelial METRNL deficiency accelerates atherosclerosis in ApoE^{-/-} mice

To determine whether or not endothelial METRNL deficiency affects the development of atherosclerosis, EC-Metrnl^{-/-} mice

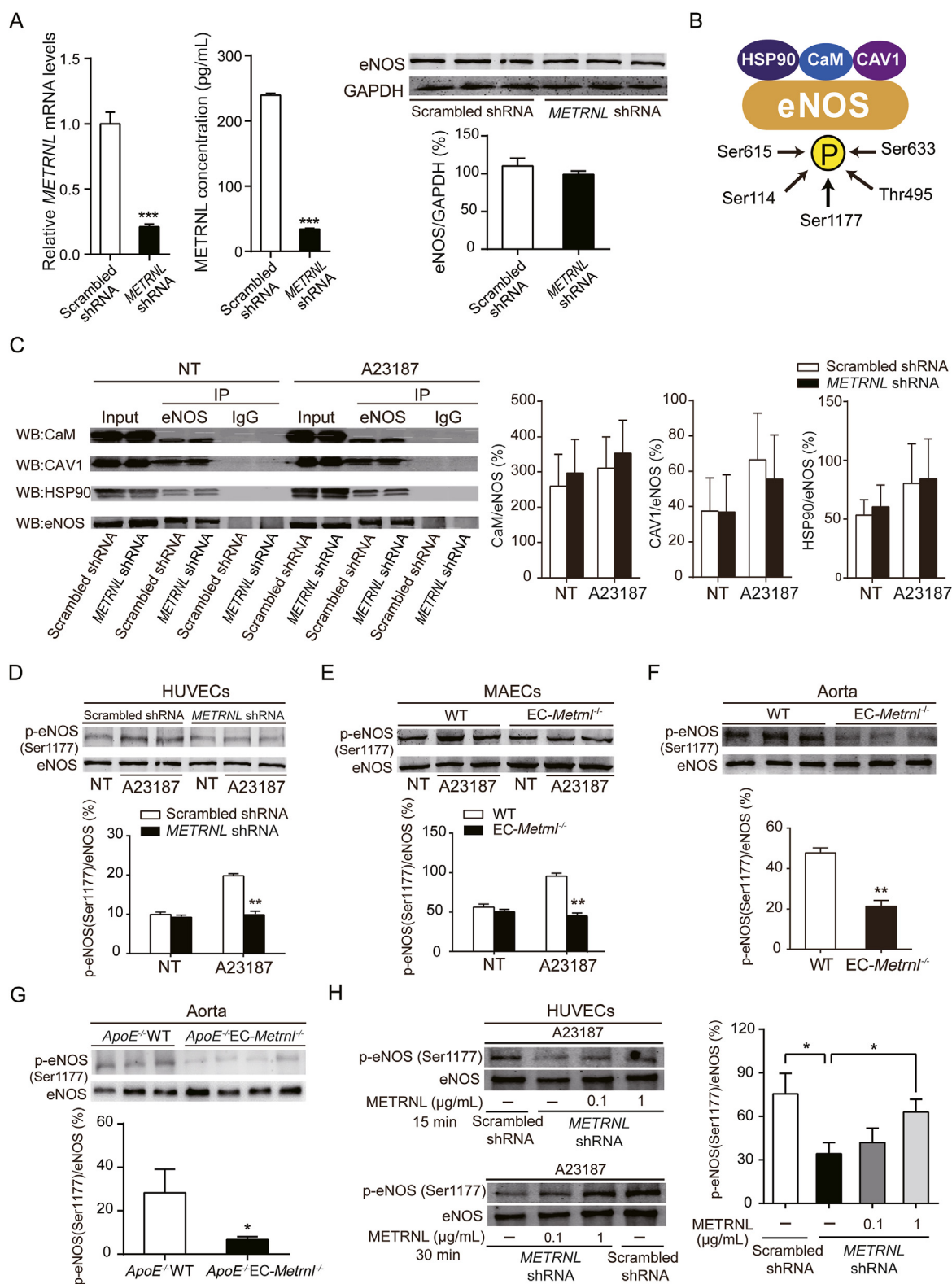


Figure 7 METRNL deficiency reduces eNOS phosphorylation at Ser1177. (A) eNOS protein level in HUVECs with lentivirus-mediated *METRNL* knockdown (*METRNL* shRNA) or vehicle (Scrambled shRNA) ($n = 3$). (B) Working model of eNOS interacted proteins and eNOS phosphorylations involved in eNOS activity. (C) The interactions between eNOS and calmodulin (CaM), caveolin-1 (CAV1), or heat shock protein 90 (HSP90), detected by immunoprecipitation in HUVECs after *METRNL* knockdown in presence or absence of eNOS activator (calcium ionophore A23187, 1 $\mu\text{mol/L}$) during 10 min ($n = 3-5$). NT, no treatment. (D-H) eNOS phosphorylation at Ser1177 in HUVECs after *METRNL* knockdown (D), in MAECs (E) and aortae (F) from *EC-Metn1*^{-/-} mice and in aortae (G) from *ApoE*^{-/-}*EC-Metn1*^{-/-} mice without atherosclerosis (3 months of age under normal chow). $n = 3-4$ per group. (H) Exogenous METRNL ameliorates reduced eNOS phosphorylation at

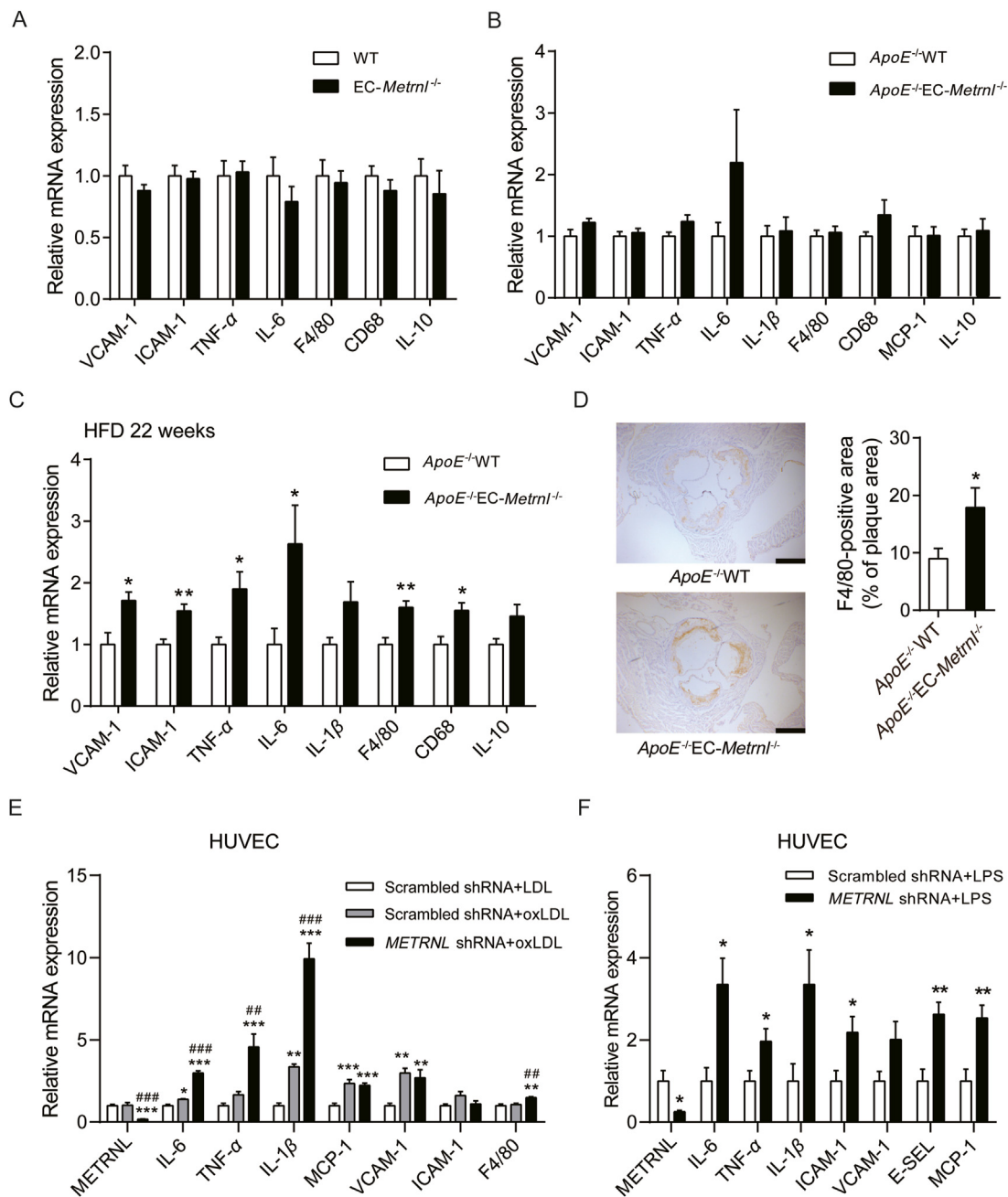


Figure 8 Endothelial METRNL deficiency aggravates endothelial inflammation during atherosclerosis. (A–C) mRNA expressions of inflammatory markers in aortae from EC-Metrnl^{-/-} mice (A, $n = 6-9$), ApoE^{-/-}EC-Metrnl^{-/-} mice at 3 months of age under normal chow without atherosclerosis (B, $n = 9-11$) and ApoE^{-/-}EC-Metrnl^{-/-} mice fed 22 weeks of HFD with obvious atherosclerosis (C, $n = 4-6$) as well as their littermates. (D) Immunohistochemical staining for F4/80 in aortic roots from ApoE^{-/-}EC-Metrnl^{-/-} and ApoE^{-/-}WT mice after 22 weeks of HFD ($n = 5$). Bar = 500 μ m. (E, F) mRNA expressions of inflammatory markers in METRNL deficient HUVECs and controls under stimulation of oxLDL (100 μ g/mL) (E, $n = 6$) or LPS (1 μ g/mL) (F, $n = 5-6$) for 24 h. LDL, low density lipoprotein; oxLDL, oxidized low density lipoprotein; LPS, lipopolysaccharide; VCAM, vascular cell adhesion molecule; ICAM, intercellular adhesion molecule; TNF, tumor necrosis factor; IL, interleukin; MCP, monocyte chemoattractant protein; CD, cluster of differentiation; E-SEL, E-selectin. Data are mean \pm SEM. * $P < 0.05$, ** $P < 0.01$, *** $P < 0.001$ by two-tailed Student's t test in (C, D and F). * $P < 0.05$, ** $P < 0.01$, *** $P < 0.001$ vs. Scrambled shRNA + LDL; ### $P < 0.01$, #### $P < 0.001$ vs. Scrambled shRNA + oxLDL by one-way ANOVA followed by Dunnett's t test in (E).

Ser1177 in METRNL-deficient HUVECs. Cells were incubated with recombinant METRNL (0.1 or 1 μ g/mL) or a solvent control (PBS) for 15 or 30 min, after which A23187 was added at 1 μ mol/L for 10 min ($n = 3-4$). Data are mean \pm SEM. * $P < 0.05$, ** $P < 0.01$, *** $P < 0.001$ by two-tailed Student's t test in (A and D–H).

were crossed with $ApoE^{-/-}$ mice to generate double knockout mice ($ApoE^{-/-}EC-Metrnl^{-/-}$); the $ApoE^{-/-}$ WT littermates were used as control (Fig. 5A and B and Fig. S2). Compared with $ApoE^{-/-}$ WT mice, both aortic *Metrnl* expression and circulating METRNL level were significantly reduced in $ApoE^{-/-}EC-Metrnl^{-/-}$ mice (Fig. 5C), with no changes in food intake, body weight, liver weight and blood glucose (Supporting Information Fig. S11). After 22 weeks of HFD, the atherosclerotic burden of the two mouse groups was assessed by ORO staining in whole aortae. The *en face* analysis revealed significantly larger sizes of atherosclerotic lesions in aortae of double knockout mice than in $ApoE^{-/-}$ WT preparations (Fig. 5D and E). To further visualize lesions in the aortic roots, hematoxylin and eosin staining and ORO staining were combined. The double knockout mouse group had more lipid deposition within the atherosclerotic plaque, with larger hematoxylin and eosin-negative acellular area indicating more severe necrotic cores (Fig. 5F), as well as larger atherosclerotic lesions in the aortic roots (Fig. 5G). Spontaneous atherosclerosis at the age of one year was also more severe in $ApoE^{-/-}EC-Metrnl^{-/-}$ mice than $ApoE^{-/-}$ WT littermates under normal chow diet (Fig. 5H). Further, early atherosclerosis was induced by a relatively short period (10 weeks) of HFD, and more obvious lesion was also observed in aortae of $ApoE^{-/-}EC-Metrnl^{-/-}$ than $ApoE^{-/-}$ WT mice (Fig. 5I). All these results indicate that endothelial METRNL deficiency accelerates the occurrence and development of atherosclerosis.

3.6. Endothelial METRNL deficiency impairs endothelium-dependent vascular relaxation through reducing eNOS phosphorylation at Ser1177, rescued by exogenous METRNL

Endothelial dysfunction manifested by impaired endothelium-dependent vascular relaxation has been proposed as the first step toward or at least an early marker of atherosclerosis^{17,30–33}. To determine whether or not endothelial METRNL deficiency affects endothelium-dependent vascular relaxation, isolated mouse aortae were used in the present study. Phe-induced aortic contractions were comparable in preparations of $EC-Metrnl^{-/-}$ and wild type mice. However, relaxations to the endothelium-dependent vasodilator ACh were significantly attenuated in aortae of $EC-Metrnl^{-/-}$ mice (Fig. 6A); by contrast, those to the endothelium-independent vasodilator SNP were unchanged (Fig. 6B). Consistently, similar phenomena were observed in aortae from $ApoE^{-/-}EC-Metrnl^{-/-}$ mice and $ApoE^{-/-}$ WT mice (Fig. 6D and E) at 3 months of age under normal chow without atherosclerosis (Fig. 6F). Moreover, the significantly attenuated ACh-induced relaxation in aortae of $ApoE^{-/-}EC-Metrnl^{-/-}$ mice were successfully rescued by exogenous administration of recombinant METRNL protein (Fig. 6D). Simultaneously, serum levels of lipids including total cholesterol (TC), triglycerides (TG), high density lipoprotein-cholesterol (HDL-C), low density lipoprotein-cholesterol (LDL-C), and nonesterified fatty acids (NEFA) were unchanged in $EC-Metrnl^{-/-}$ mice (Fig. 6C), $ApoE^{-/-}EC-Metrnl^{-/-}$ mice without atherosclerosis (3 months of age under normal chow, Fig. 6G), $ApoE^{-/-}EC-Metrnl^{-/-}$ mice with mild atherosclerosis (10 weeks of HFD, Fig. 6H) and severe atherosclerosis (22 weeks of HFD, Fig. 6I), compared with their littermate controls. All these results indicate that endothelial METRNL deficiency impairs endothelium-dependent vascular relaxation before the occurrence of atherosclerosis. And this endothelial dysfunction triggered by METRNL deficiency is probably a key

factor responsible for the more severe atherosclerosis in double knockout mice.

Further, the underlying molecular mechanism was studied. In conduit arteries such as the aorta, endothelium-dependent relaxations to ACh are due to activation of endothelial nitric oxide synthase (eNOS), since both pharmacological inhibition and gene knockout of eNOS abolish the response to ACh^{17,18,32,34–36}. Thus, METRNL deficiency-induced endothelial vasodilation dysfunction in the present experiments can be attributed to impairment of the eNOS pathway. To know the role of METRNL in the regulation of eNOS, *in vitro* experiments were performed. *METRNL* knockdown by lentivirus-mediated shRNA interference in HUVECs significantly reduced METRNL level in the cell and culture medium, but did not alter eNOS protein level (Fig. 7A), suggesting that the quantity of eNOS is not regulated by METRNL.

Then, eNOS-related activity was examined (Fig. 7B). Protein-interactions play a crucial role in the regulation of eNOS activity^{32,37}. For example, caveolin-1 (CAV1) inhibits eNOS function, while heat shock protein 90 (HSP90) and calmodulin (CaM) enhance the activity of the enzyme. Hence, the interactions between eNOS and CAV1, HSP90 or CaM were determined by immunoprecipitation at baseline or following activation of eNOS by A23187. No significant changes were observed in the amount of eNOS-combined CAV1, HSP90 or CaM in METRNL-deficient HUVECs compared with control HUVECs (Fig. 7C), suggesting that METRNL does not regulate the interactions of eNOS with CAV1, CaM or HSP90.

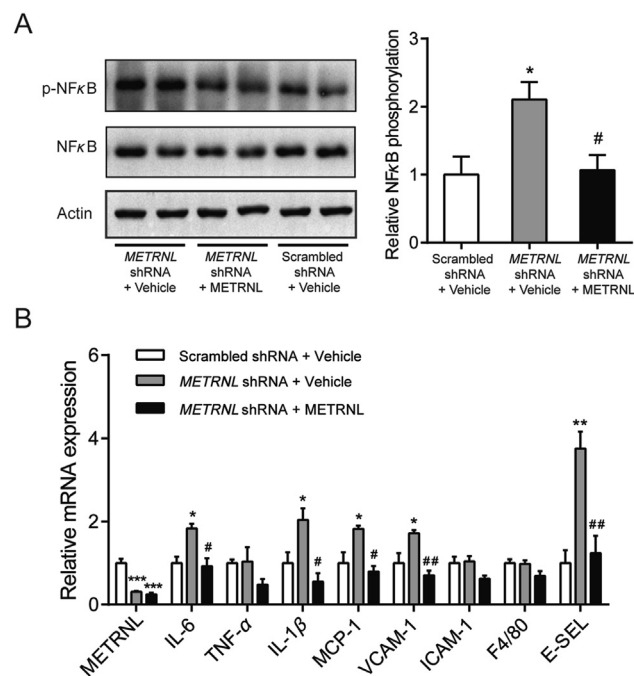


Figure 9 Endothelial METRNL deficiency aggravates endothelial inflammation via NFκB pathway. Cells were incubated with recombinant METRNL (300 ng/mL) or vehicle (PBS) for 1 h before stimulation by oxLDL (100 μg/mL) for 24 h. (A) NFκB p65 phosphorylation levels in HUVECs ($n = 3-4$). (B) mRNA expressions of inflammatory markers in HUVECs ($n = 3$). Data are mean \pm SEM. * $P < 0.05$, ** $P < 0.01$, *** $P < 0.001$ vs. Scrambled shRNA + vehicle; # $P < 0.05$, ## $P < 0.01$ vs. *METRNL* shRNA + vehicle by one-way ANOVA followed by Dunnett's *t* test in (A, B).

Phosphorylation is the most important post-translational mechanism modulating eNOS activity (Fig. 7B)^{32,38}. There are five established serine/threonine phosphorylation sites (Ser1177, Ser633, Ser114, Thr495, and Ser615) in human eNOS^{32,38}. Thus, the effect of METRNL deficiency on eNOS phosphorylations was

determined in HUVECs. There were no significant differences in phosphorylations of eNOS at Ser633, Ser114, Ser615 and Thr495 between cells treated with either scrambled shRNA control or *METRNL* shRNA, in either the presence or the absence of stimulation with A23187 (Supporting Information Fig. S12).

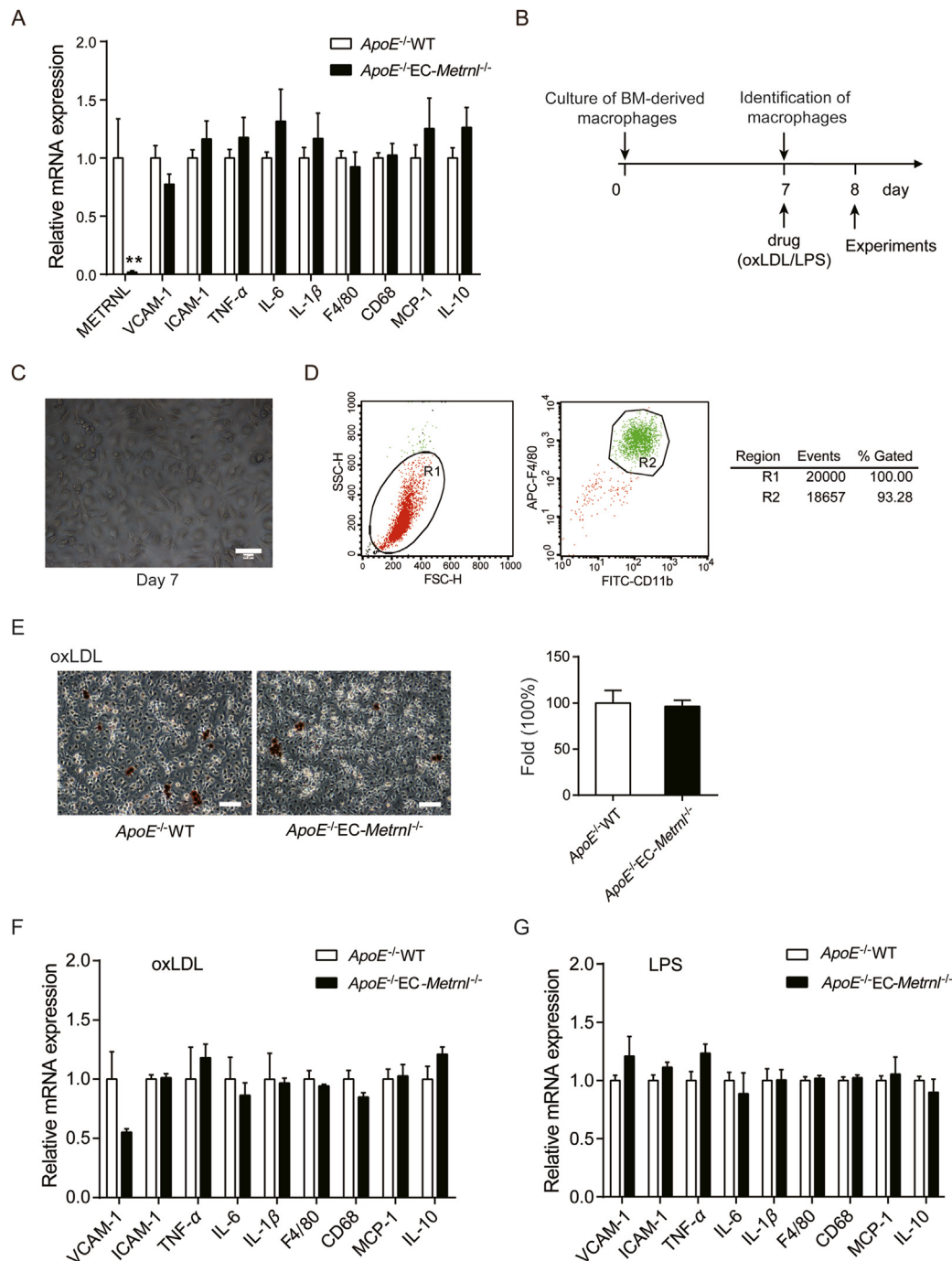
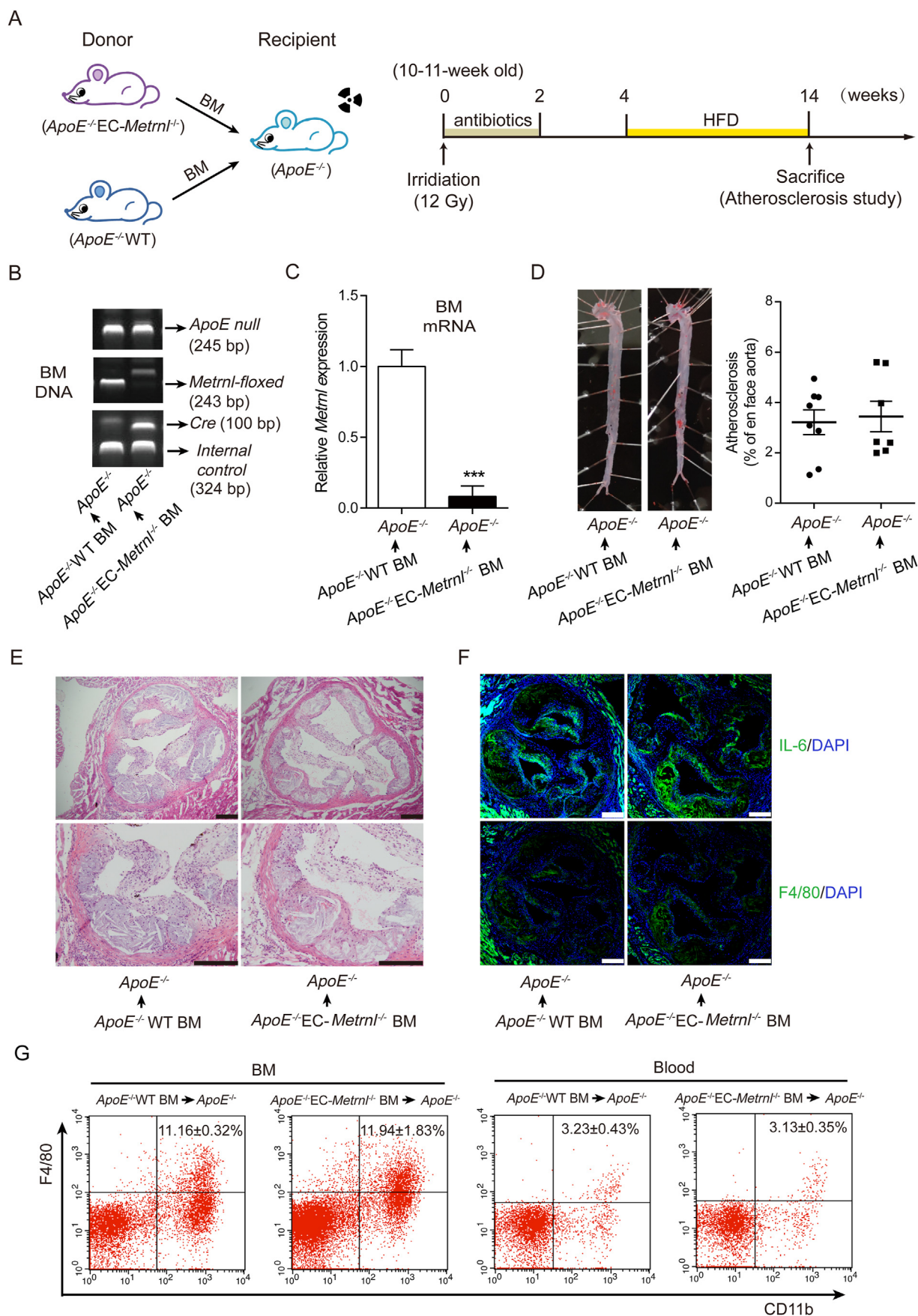


Figure 10 Effects of METRNL deficiency on inflammation of BM cells and BM-derived macrophages from *ApoE*^{-/-}EC-*Metrnl*^{-/-} mice and littermates at 3 months of age. (A) mRNA expressions of inflammatory markers in BM cells from *ApoE*^{-/-}EC-*Metrnl*^{-/-} mice and littermates ($n = 6-8$). (B) Treatment design of BM-derived macrophages. (C) Cultured macrophages at day 7 under optical microscopy. Bar = 50 μ m. (D) Identification of macrophages by flow cytometry at day 7 of culture. (E) ORO staining for macrophages ($n = 6$) after 24 h of oxLDL (50 μ g/mL) stimulation. Lipid-laden macrophages were stained red (left) and the percentages of ORO-positive cells were compared (right). (F, G) mRNA expressions of inflammatory markers in BM-derived macrophages under stimulation of oxLDL (50 μ g/mL) (F, $n = 6$) or LPS (100 ng/mL) (G, $n = 5-6$) for 24 h. Data are mean \pm SEM. ** $P < 0.01$, *** $P < 0.001$ by two-tailed Student's t test in (A, F).



However, phosphorylation of eNOS at Ser1177 was significantly reduced by *METRNL* knockdown in the presence of A23187 (Fig. 7D). Consistently, a similar phenomenon was observed in primary cultured murine aortic endothelial cells from EC-*Metnl*^{-/-} and wild type mice (Fig. 7E). Moreover, phosphorylation of eNOS at Ser1177 was also reduced in aortae of EC-*Metnl*^{-/-} mice (Fig. 7F) and *ApoE*^{-/-}EC-*Metnl*^{-/-} mice without atherosclerosis (3 months of age under normal chow) (Fig. 7G), compared with their littermate controls. More importantly, the reduced phosphorylation of eNOS at Ser1177 in *METRNL* deficient HUVECs was ameliorated by *METRNL* recombinant protein (Fig. 7H). These results indicate that endothelial *METRNL* deficiency impairs eNOS activity by reducing phosphorylation of the enzyme at Ser1177, which can be rescued by exogenous *METRNL*.

3.7. Endothelial *METRNL* deficiency aggravates endothelial inflammation during atherosclerosis through NFκB pathway, rescued by exogenous *METRNL*

Atherosclerosis is a chronic inflammatory disease in the initiation of which cytokines play a major role^{30,31,33}. To examine whether endothelial *METRNL* deficiency induces vascular inflammation, aortae from EC-*Metnl*^{-/-} mice, *ApoE*^{-/-}EC-*Metnl*^{-/-} mice without atherosclerosis (3 months of age) or with obvious atherosclerosis (22 weeks of HFD) and their littermates were used to analyze the expressions of pro-inflammatory markers³⁹ such as vascular cell adhesion molecule (VCAM)-1, intercellular adhesion molecule (ICAM)-1 and monocyte chemoattractant protein (MCP)-1 (endothelial adhesion molecules), F4/80 and CD68 (macrophage indicators), tumor necrosis factor (TNF)-α, interleukin (IL)-1β and IL-6 (general inflammatory factors), and anti-inflammatory marker IL-10. The expression levels of all examined cytokines were comparable in the aortae of EC-*Metnl*^{-/-} mice and their controls (Fig. 8A). Pro-inflammatory factors such as VCAM-1, TNF-α, IL-6 and CD68 showed a trend to increase but with no significant differences in the aortae of *ApoE*^{-/-}EC-*Metnl*^{-/-} mice without atherosclerosis compared with their controls (Fig. 8B). However, aortae from *ApoE*^{-/-}EC-*Metnl*^{-/-} mice with obvious atherosclerosis (22 weeks of HFD) exhibited elevations in expressions of pro-inflammatory markers including VCAM-1, ICAM-1, F4/80, CD68, TNF-α and IL-6, but not of the anti-inflammatory marker IL-10 (Fig. 8C). Immunohistochemical staining also showed that F4/80 and IL-6 were increased in aortic roots of *ApoE*^{-/-}EC-*Metnl*^{-/-} mice (Fig. 8D and Supporting Information Fig. S13). These results further support more severe atherosclerosis in the aortae of the double knockout mice and suggest that endothelial *METRNL* deficiency promotes vascular inflammation during atherosclerosis development rather than before the initial stage of the disease.

During atherosclerosis development, several pro-inflammatory factors in serum such as oxidized low-density lipoprotein (oxLDL) activates endothelial cells to release several cytokines, which recruit circulating monocytes and leukocyte, thereby promoting inflammation within the vessel wall⁴⁰. To further analyze the effect of *METRNL* deficiency on endothelial inflammation during atherosclerosis, *in vitro* experiments were performed. Under stimulation of oxLDL, pro-inflammatory factors including IL-6, TNF-α and IL-1β were significantly increased in *METRNL* knockdown group (Fig. 8E). Similarly, lipopolysaccharide (LPS) also triggered more severe endothelial inflammation in *METRNL* deficient group (Fig. 8F). These observations suggest that the aggravated endothelial inflammation induced by *METRNL* deficiency is another contributor to the more severe atherosclerosis in *ApoE*^{-/-}EC-*Metnl*^{-/-} mice than control mice.

Since the nuclear transcription factor-kappa B (NFκB) is a critical inflammatory transcription factor, we next explored whether the NFκB pathway mediates the inflammation response in *METRNL* deficient HUVECs under oxLDL stimulation. The protein level of NFκB p65 was determined by Western blotting. The p65 phosphorylation was significantly increased after oxLDL stimulation in *METRNL* deficient HUVECs, but was attenuated by exogenous administration of *METRNL* recombinant protein (Fig. 9A). Consistently, at mRNA levels, exogenous *METRNL* successfully attenuated the oxLDL-induced increase of the inflammatory markers in *METRNL* deficient HUVECs, including IL-6, IL-1β, MCP-1, VCAM-1 and E-selectin (E-SEL) (Fig. 9B). All these suggest an anti-inflammatory role of endothelial *METRNL* *via* inhibition of NFκB pathway activation.

3.8. Bone marrow *METRNL* deficiency does not change the occurrence of atherosclerosis

It has been recognized that BM hematopoietic cells play a role in the occurrence of atherosclerosis¹⁶. As shown in Fig. 3G, *METRNL* expression was reduced in BM cells of EC-*Metnl*^{-/-} mice. Thus, to know whether ablation of *METRNL* in BM cells contributes to the detrimental atherosclerotic phenotype observed in *ApoE*^{-/-}EC-*Metnl*^{-/-} mice, BM cells were isolated from the mice to carry out a series of experiments. Real time PCR analysis of BM cells from 3-month-old *ApoE*^{-/-}EC-*Metnl*^{-/-} mice and their littermate controls showed comparable expression levels of pro-inflammatory factors such as VCAM-1, ICAM-1, TNF-α, IL-6, IL-1β, F4/80, CD68 and MCP-1, and anti-inflammatory factor IL-10 (Fig. 10A). Mouse BM-derived macrophages were isolated and cultured (Fig. 10B). At day 7 of culture (named M0 macrophages, Fig. 10C), over 90% of the cells were CD11b and F4/80 positive (Fig. 10D). To induce formation of foam cell, the macrophages were incubated with oxLDL (50 μg/mL) for 24 h

Figure 11 Deficiency of *METRNL* in BM cells does not change the occurrence of atherosclerosis. (A) Design of BM transplantation and atherosclerosis experiments. (B) Genotype of BM DNA after transplantation. (C) *Metnl* mRNA expression in BM of chimeric *ApoE*^{-/-} mice receiving donor BM cells from *ApoE*^{-/-}EC-*Metnl*^{-/-} or *ApoE*^{-/-}WT mice ($n = 5-8$). (D) Atherosclerotic lesions in aortae from chimeric *ApoE*^{-/-} mice receiving donor BM cells from *ApoE*^{-/-}EC-*Metnl*^{-/-} or *ApoE*^{-/-}WT mice after HFD for 10 weeks ($n = 7-8$). (E) Hematoxylin and eosin staining of aortic roots from chimeric *ApoE*^{-/-} mice receiving donor BM cells from *ApoE*^{-/-}EC-*Metnl*^{-/-} or *ApoE*^{-/-}WT mice after HFD for 10 weeks. Bar = 200 μm. Five independent experiments performed. (F) IL-6 and F4/80 staining of aortic roots from chimeric *ApoE*^{-/-} mice receiving donor BM cells from *ApoE*^{-/-}EC-*Metnl*^{-/-} or *ApoE*^{-/-}WT mice after HFD for 10 weeks. Bar = 200 μm. Four independent experiments performed. (G) Flow cytometric analysis of F4/80 and CD11b expression on cell samples isolated from BM ($n = 5-7$) and peripheral blood ($n = 3-6$) from chimeric *ApoE*^{-/-} mice receiving donor BM cells from *ApoE*^{-/-}EC-*Metnl*^{-/-} or *ApoE*^{-/-}WT mice after HFD for 10 weeks. Data are mean ± SEM. *** $P < 0.001$ by two-tailed Student's t test in (C).

and stained by ORO, demonstrating that oxLDL successfully resulted in foam cell formation in macrophages from *ApoE*^{-/-} EC-*Metrn1*^{-/-} mice and littermates, whereas no difference was observed in percentages of ORO-positive cells between them (Fig. 10E). Meanwhile, macrophages derived from these two mouse groups with oxLDL (50 µg/mL) or LPS (100 ng/mL) stimulation for 24 h were examined; consistently, in the expressions of pro-inflammatory and anti-inflammatory factors, no significant difference was observed between the two groups (Fig. 10F and G).

To further explore the effect of bone marrow METRNL deficiency on the occurrence of atherosclerosis, BM transplantation and atherosclerosis experiments were carried out (Fig. 11A). The chimeric mice were made by the recipient atherosclerosis model mice (*ApoE*^{-/-} mice) being given donor BM cells from *ApoE*^{-/-} EC-*Metrn1*^{-/-} mice or *ApoE*^{-/-} WT littermate control mice (Fig. 11A). Identified by genotyping of BM DNA, BM cells of the recipient *ApoE*^{-/-} mice were successfully replaced by those from donor mice (Fig. 11B). *Metrn1* was efficiently depleted in BM of chimeric *ApoE*^{-/-} mice receiving *ApoE*^{-/-} EC-*Metrn1*^{-/-} BM cells (Fig. 11C). After HFD for 10 weeks, atherosclerotic lesions in *ApoE*^{-/-} recipient mice transplanted with BM cells from *ApoE*^{-/-} EC-*Metrn1*^{-/-} or littermate control mice were examined. The results showed comparable atherosclerotic plaque burden in aortae of these two groups (Fig. 11D), and no difference was observed in lesion severity (Fig. 11E) and inflammation (Fig. 11F) of the aortic roots between them. Flow cytometric analysis of F4/80 and CD11b expression on cell samples isolated from peripheral blood and BM from the two groups of chimeric *ApoE*^{-/-} mice revealed no difference in frequencies of macrophages (Fig. 11G), a kind of cells believed to play an important role in the development of atherosclerosis including lipid handling and inflammatory functions¹⁶. These findings indicate that deficiency of METRNL in BM cells is not involved in acceleration of atherosclerosis occurrence in *ApoE*^{-/-} EC-*Metrn1*^{-/-} mice.

4. Discussion

The present study reveals that METRNL is a new endothelial substance not only determining the circulating level of the protein but also regulating endothelial function for vascular homeostasis.

4.1. Circulating METRNL mainly originates from endothelial cells and is associated with atherosclerosis

Our previous studies have demonstrated that METRNL is highly present in human and murine white adipocytes and intestinal epithelial cells and can be released from these cells and tissues^{4,5,7}. However, specific knockout of *Metrn1* in either adipocytes or intestinal epithelial cells does not significantly change the serum METRNL levels, indicating that circulating METRNL is not mainly derived from these two types of cells^{5,7}. Although liver is the major source of blood protein, the presence of METRNL in the liver is very low and specific knockout of liver *Metrn1* also does not alter circulating METRNL levels in our recent study⁴¹. The present study identified endothelium as the main origin of circulating METRNL by showing that METRNL was highly present in and secreted by endothelial cells, and more importantly, endothelium-specific knockout of *Metrn1* resulted in a reduction of serum METRNL level by about 75%. It has been considered that *Tek-Cre* promoter results in specific target deletion in not only

endothelial cells but also hematopoietic cells²⁹. However, our study showed that METRNL expression in BM was very low in normal conditions and the BM transplantation study demonstrated that BM METRNL deficiency mediated by *Tek-Cre* did not affect the serum METRNL levels. Therefore, the potential contribution of BM hematopoietic cells to circulating METRNL level is neglected in EC-*Metrn1*^{-/-} mice, further supporting that the endothelium is the major contributor of circulating METRNL.

There are classical and non-classical secretory pathways responsible for cell release of proteins. A signal peptide is predicted with cleavage between the 45th and 46th amino acids of METRNL by bioinformatic analysis⁴, suggesting that the protein may be secreted *via* a classical secretory pathway, but evidence confirming this is lacking. We showed that METRNL secretion was efficiently regulated by its gene overexpression and knock-down, with a requirement for its signal peptide. This signal peptide-guided secretion of the protein is a characteristic for the classical ER–Golgi secretion pathway. Further, the present findings demonstrated that METRNL was secreted by endothelial cells *via* the classical secretory pathway using pharmacological inhibitors targeting conventional ER–Golgi pathway. This is also supported by the evidence for METRNL presence in ER and Golgi apparatus.

The results that circulating METRNL mainly originates from endothelial cells also suggest that circulating METRNL level reflects the vascular state, especially the condition of endothelium. Atherosclerosis is a vascular disease with endothelial dysfunction and damage, which may affect METRNL production resulting in a reduction of circulating METRNL levels. Indeed, the present study found reduced circulating METRNL level in both atherosclerosis mice and humans, and the protein level was associated with the atherosclerosis situation; METRNL protein levels were reduced in the circulation and endothelium of atherosclerosis mice, with much more reduction in more severe extents of atherosclerosis. All these results indicate that circulating METRNL reduction exists in atherosclerosis state. Perhaps, METRNL may be a circulating biomarker for atherosclerosis.

In line with our present study in atherosclerosis animals and humans, recent clinical studies also showed that lower circulating METRNL levels were associated with type 2 diabetes mellitus and coronary artery disease^{13,14,42,43} which are well-known accompanied by endothelial damage and dysfunction. However, all these clinical studies^{13,14,42,43} including our previous research¹³ did not know the cause of the lower circulating METRNL levels in these diseases, and the investigators focused on METRNL/Subfatin as an adipokine. The present finding that circulating METRNL is mainly derived from endothelial cells provides a novel insight for understanding why circulating METRNL levels decrease in these patients. METRNL may be a circulating biomarker for certain vascular disease with endothelial damage and dysfunction, which remains to be further studied. Also, in clinical study, a more precise estimation on circulating METRNL levels is of particular note, since the level of METRNL in circulation is very likely to fluctuate with physiological states. For example, it is associated with inflammatory responses *in vivo*¹¹ and other influence factors may include drugs, physical exercise, cold exposure and so on⁴⁴.

4.2. METRNL deficiency causes endothelial dysfunction and accelerates atherosclerosis

Using a double gene knockout strategy by *Tek-Cre* mediated *Metrn1* deletion in *ApoE* deficient mice, the present study

demonstrated that endothelial METRNL deficiency accelerated the occurrence and development of atherosclerosis, evidenced by three sets of experiments in *ApoE*^{-/-}*EC-Metrnl*^{-/-} mice with different periods (10 or 22 weeks) of HFD, or spontaneous atherosclerosis at one year of age under normal chow. Regarding the mechanisms underlying the acceleration of atherosclerosis by endothelial METRNL deficiency, several major factors have been investigated in the present study.

First, it has been recognized that dyslipidemia is a principal risk factor for atherosclerosis^{17,33}. However, this mechanism seems not to be involved in the acceleration of atherosclerosis by METRNL deficiency, since *Tek-Cre* mediated knockout of *Metrnl* did not change the blood levels of lipids including TC, TG, HDL-C, LDL-C and NEFA, no matter whether *ApoE* was deficient or not, and no matter whether HFD was given or not.

Second, endothelial dysfunction manifested by impairment of endothelium-dependent vasodilation has been proposed as the first step toward or at least as an early marker of atherosclerosis^{17,30–33}. The present experiments in isolated aortae showed that endothelial METRNL deficiency attenuated relaxations to the endothelium-dependent vasodilator ACh, without affecting relaxations to endothelium-independent vasodilator SNP. This endothelium-dependent vasodilation dysfunction occurred not only in single gene knockout mice (*EC-Metrnl*^{-/-} mice) but also in double gene knockout mice (*ApoE*^{-/-}*EC-Metrnl*^{-/-} mice) before the occurrence of atherosclerosis, further supporting the notion that endothelial dysfunction can occur well before the structural manifestation of atherosclerosis and thus can serve as an independent predictor of future cardiovascular events⁴⁰. Regarding the molecular mechanism, we have screened and identified that the impaired eNOS phosphorylation at Ser1177 is involved in METRNL deficiency induced endothelial vasodilation dysfunction, which can be rescued by exogenous METRNL.

Third, inflammation is a key element in the development of atherosclerosis^{45–47}. There existed no significant inflammation activation in the aortae of both *EC-Metrnl*^{-/-} mice and *ApoE*^{-/-}*EC-Metrnl*^{-/-} mice before the occurrence of atherosclerosis. However, the present study clearly demonstrated that the expressions of inflammatory factors were activated in *ApoE*^{-/-}*EC-*

Metrnl^{-/-} mice during atherosclerosis. This further supports the more severe atherosclerosis in the aortae of the double knockout mice and suggest that endothelial METRNL deficiency promotes vascular inflammation during atherosclerosis development rather than before the initial stage of the disease. Further, in primary cultured endothelial cells with *METRNL* knockdown, we indeed observed more severe endothelial inflammation compared with control group under stimulation of oxLDL or LPS. This aggravation in endothelial inflammation may involve NFκB pathway activation by *METRNL* knockdown, which can be rescued by exogenous METRNL. These endothelial dysfunction data on inflammation activation combined with the endothelial dysfunction data on vasodilation impairment indicate that endothelial dysfunction plays a major role in acceleration of atherosclerosis by METRNL deficiency, in which endothelial vasodilation impairment occurs earlier than endothelial inflammation activation.

Forth, since *Tek-Cre* also mediated reduced METRNL level in BM cells which potentially contributes to atherosclerosis, we performed a series of *in vivo* and *in vitro* experiments for clarification. There existed also no inflammation activation in BM of *ApoE*^{-/-}*EC-Metrnl*^{-/-} mice before the occurrence of atherosclerosis. BM-derived macrophages from *ApoE*^{-/-}*EC-Metrnl*^{-/-} mice and their littermates showed no difference in foam cell formation, and under either oxLDL or LPS stimulation, the two groups showed similar expression levels of inflammatory factors. More importantly, using BM transplantation strategy to produce BM-specific intervention model, the present study showed that BM METRNL deficiency in *ApoE*^{-/-} mice did not change the occurrence and severity of atherosclerotic lesion as well as inflammation in BM and peripheral blood. Thus, the possibility for BM METRNL deficiency in accelerating atherosclerosis is excluded, further supporting that it is the endothelial METRNL deficiency responsible for the acceleration of atherosclerosis in *ApoE*^{-/-}*EC-Metrnl*^{-/-} mice.

Therefore, according to the above mechanism study, it appears that endothelial METRNL deficiency causes vascular endothelial dysfunction such as vasodilation impairment *via* reducing eNOS phosphorylation and inflammation activation *via* enhancing NFκB

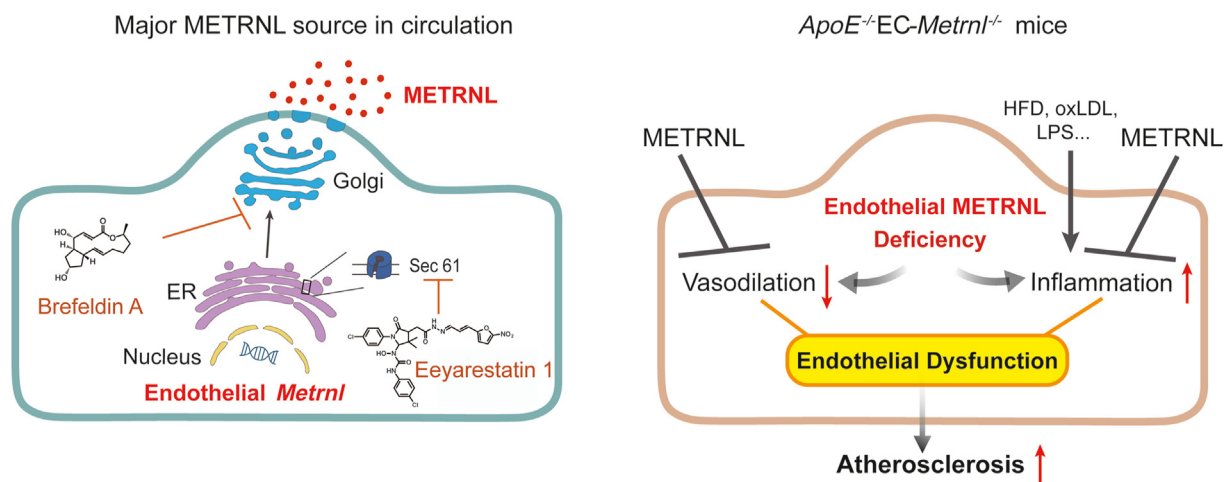


Figure 12 Endothelial METRNL is not only a major source for circulating METRNL but also a novel regulator in vascular health and disease. Using the classical endoplasmic reticulum (ER)–Golgi apparatus secretory pathway, endothelial cells secrete and, hence, determine the circulating level of METRNL, the deficiency of which causes endothelial dysfunction promoting the occurrence and development of atherosclerosis. Recombinant METRNL can rescue the endothelial dysfunction induced by METRNL deficiency.

pathway, then favoring the occurrence and development of atherosclerosis. And, endothelial METRNL itself is atheroprotective and plays a critical role in the maintenance of vascular health. This is also supported by our present results that recombinant METRNL can rescue the METRNL deficiency induced endothelial dysfunction including the impairment of vasodilation and eNOS phosphorylation as well as the activation of inflammation and NF κ B pathway. Other report also shows that recombinant METRNL can inhibit the LPS-induced endothelial inflammation and attachment with monocytes in *in vitro* cell lines culture⁴⁸. These indicate that recombinant METRNL has a therapeutic effect for the METRNL deficiency induced endothelial dysfunction, and may have a beneficial effect on prevention and treatment of atherosclerosis. Given that endothelial cells are sentinels of cardiovascular health, and endothelial dysfunction is a hallmark of many diseases, including atherosclerosis, hypertension, coronary artery disease, cerebrovascular disease, peripheral vascular disease, and diabetes^{32,36}, the present study on the discovery of METRNL as a new endothelium-derived protective factor is of importance for further study to explore the therapeutic strategy of METRNL. As for further understanding the therapeutic potential of METRNL in the chronic disease of atherosclerosis, double gene mice with *Metrl* transgenic overexpression and *ApoE* gene knockout are the better model for the future study.

In addition to the vascular protection of METRNL in the present study, METRNL exhibits beneficial functions in metabolic and inflammatory diseases⁴⁴. Our previous works also show that METRNL improves HFD induced insulin resistance and inflammation at least partly through remodeling adipose tissue⁵. Moreover, METRNL is upregulated in inflammatory diseases, such as rheumatoid arthritis, allergic asthma, etc., and plays an anti-inflammatory role^{49,50}. For instance, METRNL attenuates HFD associated inflammation in both adipose tissue and skeletal muscle^{5,9} and decreases inflammatory cell infiltration and pro-inflammatory mediators production in chronic colitis and allergic asthma^{49,50}, apart from its inhibitory effects on endotoxin induced inflammation responses in endothelial cells⁴⁸. In several disorders including insulin resistance^{5,9}, diabetes^{51,52}, chronic colitis⁵⁰, and allergic asthma⁴⁹, METRNL gene and/or protein demonstrate a therapeutic potential. Considering that metabolic disorder and inflammation are both involved in the development of cardiovascular disease, these results indicate that METRNL could be a multifaceted therapeutic target in cardiovascular diseases.

5. Conclusions

In summary, the present study demonstrates that METRNL is a new endothelial substance. Endothelial METRNL is not only a major source of circulating METRNL, but also an important regulator of endothelial function for vascular health and disease (Fig. 12). Both endothelial and circulating METRNL levels decrease in disease state of atherosclerosis. METRNL deficiency causes endothelial dysfunction which in turn promotes the susceptibility of atherosclerosis. Overall, the present findings reveal that METRNL is a therapeutic target against endothelial dysfunction and atherosclerosis.

Acknowledgments

The authors appreciate Prof. Paul M. Vanhoutte (The University of Hong Kong, Hong Kong, China)'s contribution on preparing the

manuscript and data analysis. This work was supported by grants from the National Natural Science Foundation of China Major Project (Nos. 81730098 and 82030110) and National Natural Science Foundation of China Young Program (No. 82104165), Shanghai Science and Technology Commission Project (No. 201409004600, China), Shanghai Sailing Program (No. 21YF1457600, China), and Medical Innovation Project (Nos. 16CXZ009, 16QNP087 and 2018-CGPZ-A03, China).

Author contributions

Chaoyu Miao conceived and coordinated the project, designed the study, assembled and analyzed the data, and prepared the manuscript. Sili Zheng, Zhiyong Li, Jie Song, Pin Wang, and Jian Xu designed and performed most of the experiments, collected and analyzed the data, and contributed to preparing the manuscript. Wenjun Hu, Yi Shi, Qi Qi, Zhuwei Miao, and Yunfeng Guan carried out some experiments and contributed to data collection and analysis. All authors approved the final manuscript.

Conflicts of interest

The authors declare no conflicts of interest.

Appendix A. Supporting information

Supporting data to this article can be found online at <https://doi.org/10.1016/j.apsb.2022.12.008>.

References

- Kaiser J. Aging. 'Rejuvenation factor' in blood turns back the clock in old mice. *Science* 2014;**344**:570–1.
- Fasshauer M, Bluher M. Adipokines in health and disease. *Trends Pharmacol Sci* 2015;**36**:461–70.
- Zheng SL, Li ZY, Song J, Liu JM, Miao CY. Metrl: a secreted protein with new emerging functions. *Acta Pharmacol Sin* 2016;**37**:571–9.
- Li ZY, Zheng SL, Wang P, Xu TY, Guan YF, Zhang YJ, et al. Subfatin is a novel adipokine and unlike meteorin in adipose and brain expression. *CNS Neurosci Ther* 2014;**20**:344–54.
- Li ZY, Song J, Zheng SL, Fan MB, Guan YF, Qu Y, et al. Adipocyte Metrl antagonizes insulin resistance through PPAR γ signaling. *Diabetes* 2015;**64**:4011–22.
- Jorgensen JR, Fransson A, Fjord-Larsen L, Thompson LH, Houchins JP, Andrade N, et al. Cometin is a novel neurotrophic factor that promotes neurite outgrowth and neuroblast migration *in vitro* and supports survival of spiral ganglion neurons *in vivo*. *Exp Neurol* 2012;**233**:172–81.
- Li ZY, Fan MB, Zhang SL, Qu Y, Zheng SL, Song J, et al. Intestinal Metrl released into the gut lumen acts as a local regulator for gut antimicrobial peptides. *Acta Pharmacol Sin* 2016;**37**:1458–66.
- Rao RR, Long JZ, White JP, Svensson KJ, Lou J, Lokurkar I, et al. Meteorin-like is a hormone that regulates immune–adipose interactions to increase beige fat thermogenesis. *Cell* 2014;**157**:1279–91.
- Jung TW, Lee SH, Kim HC, Bang JS, Abd El-Aty AM, Hacimüftüoğlu A, et al. METRNL attenuates lipid-induced inflammation and insulin resistance via AMPK or PPAR δ -dependent pathways in skeletal muscle of mice. *Exp Mol Med* 2018;**50**:1–11.
- Miao CY, Li ZY, Miao ZW, inventors. Application of Metrl protein or gene in treating pyemia. China patent ZL201610143110.2. 2017 Sep 22.
- Ushach I, Arrevillaga-Boni G, Heller GN, Pone E, Hernandez-Ruiz M, Catalan-Dibene J, et al. Meteorin-like/Meteorin-beta is a novel

- immunoregulatory cytokine associated with inflammation. *J Immunol* 2018;**201**:3669–76.
12. Zhang SL, Li ZY, Wang DS, Xu TY, Fan MB, Cheng MH, et al. Aggravated ulcerative colitis caused by intestinal Metrnl deficiency is associated with reduced autophagy in epithelial cells. *Acta Pharmacol Sin* 2020;**41**:763–70.
 13. Zheng SL, Li ZY, Zhang Z, Wang DS, Xu J, Miao CY. Evaluation of two commercial enzyme-linked immunosorbent assay kits for the detection of human circulating Metrnl. *Chem Pharm Bull (Tokyo)* 2018;**66**:391–8.
 14. Dadmanesh M, Aghajani H, Fadaei R, Ghorban K. Lower serum levels of Meteorin-like/Subfatin in patients with coronary artery disease and type 2 diabetes mellitus are negatively associated with insulin resistance and inflammatory cytokines. *PLoS One* 2018;**13**:e0204180.
 15. Yu JG, Song SW, Shu H, Fan SJ, Liu AJ, Liu C, et al. Baroreflex deficiency hampers angiogenesis after myocardial infarction via acetylcholine- α 7-nicotinic ACh receptor in rats. *Eur Heart J* 2013;**34**:2412–20.
 16. Aparicio-Vergara M, Shiri-Sverdlov R, de Haan G, Hofker MH. Bone marrow transplantation in mice as a tool for studying the role of hematopoietic cells in metabolic and cardiovascular diseases. *Atherosclerosis* 2010;**213**:335–44.
 17. Wang P, Xu TY, Guan YF, Zhao Y, Li ZY, Lan XH, et al. Vascular smooth muscle cell apoptosis is an early trigger for hypothyroid atherosclerosis. *Cardiovasc Res* 2014;**102**:448–59.
 18. Wang P, Xu TY, Guan YF, Su DF, Fan GR, Miao CY. Perivascular adipose tissue-derived visfatin is a vascular smooth muscle cell growth factor: role of nicotinamide mononucleotide. *Cardiovasc Res* 2009;**81**:370–80.
 19. Wang P, Xu TY, Guan YF, Tian WW, Viollet B, Rui YC, et al. Nicotinamide phosphoribosyltransferase protects against ischemic stroke through SIRT1-dependent adenosine monophosphate-activated kinase pathway. *Ann Neurol* 2011;**69**:360–74.
 20. Wang JM, Chen AF, Zhang K. Isolation and primary culture of mouse aortic endothelial cells. *J Vis Exp* 2016;**118**:52965.
 21. Baudin B, Bruneel A, Bosselut N, Vaubourdolle M. A protocol for isolation and culture of human umbilical vein endothelial cells. *Nat Protoc* 2007;**2**:481–5.
 22. Shao S, Hegde RS. A calmodulin-dependent translocation pathway for small secretory proteins. *Cell* 2011;**147**:1576–88.
 23. Benham AM. Protein secretion and the endoplasmic reticulum. *Cold Spring Harbor Perspect Biol* 2012;**4**:a012872.
 24. Patterson GH, Hirschberg K, Polishchuk RS, Gerlich D, Phair RD, Lippincott-Schwartz J. Transport through the Golgi apparatus by rapid partitioning within a two-phase membrane system. *Cell* 2008;**133**:1055–67.
 25. Cross BC, McKibbin C, Callan AC, Roboti P, Piacenti M, Rabu C, et al. Eeyarestatin I inhibits Sec61-mediated protein translocation at the endoplasmic reticulum. *J Cell Sci* 2009;**122**:4393–400.
 26. Klausner RD, Donaldson JG, Lippincott-Schwartz J, Brefeldin A. Insights into the control of membrane traffic and organelle structure. *J Cell Biol* 1992;**116**:1071–80.
 27. Doms RW, Russ G, Yewdell JW, Brefeldin A redistributes resident and itinerant Golgi proteins to the endoplasmic reticulum. *J Cell Biol* 1989;**109**:61–72.
 28. Kisanuki YY, Hammer RE, Miyazaki J, Williams SC, Richardson JA, Yanagisawa M. Tie2-Cre transgenic mice: a new model for endothelial cell-lineage analysis in vivo. *Dev Biol* 2001;**230**:230–42.
 29. Payne S, De Val S, Neal A. Endothelial-specific Cre mouse models. *Arterioscler Thromb Vasc Biol* 2018;**38**:2550–61.
 30. Libby P, Ridker PM, Hansson GK. Progress and challenges in translating the biology of atherosclerosis. *Nature* 2011;**473**:317–25.
 31. Weber C, Noels H. Atherosclerosis: current pathogenesis and therapeutic options. *Nat Med* 2011;**17**:1410–22.
 32. Vanhoutte PM, Zhao Y, Xu A, Leung SW. Thirty years of saying NO: sources, fate, actions, and misfortunes of the endothelium-derived vasodilator mediator. *Circ Res* 2016;**119**:375–96.
 33. Luscher TF. Novel mechanisms of atherosclerosis and cardiovascular repair. *Eur Heart J* 2016;**37**:1709–11.
 34. Rees DD, Palmer RM, Schulz R, Hodson HF, Moncada S. Characterization of three inhibitors of endothelial nitric oxide synthase *in vitro* and *in vivo*. *Br J Pharmacol* 1990;**101**:746–52.
 35. Chataigneau T, Feletou M, Huang PL, Fishman MC, Duhault J, Vanhoutte PM. Acetylcholine-induced relaxation in blood vessels from endothelial nitric oxide synthase knockout mice. *Br J Pharmacol* 1999;**126**:219–26.
 36. Siragusa M, Thole J, Bibli SI, Luck B, Loot AE, de Silva K, et al. Nitric oxide maintains endothelial redox homeostasis through PKM2 inhibition. *EMBO J* 2019;**38**:e100938.
 37. Fleming I, Busse R. Molecular mechanisms involved in the regulation of the endothelial nitric oxide synthase. *Am J Physiol Regul Integr Comp Physiol* 2003;**284**:R1–12.
 38. Mount PF, Kemp BE, Power DA. Regulation of endothelial and myocardial NO synthesis by multi-site eNOS phosphorylation. *J Mol Cell Cardiol* 2007;**42**:271–9.
 39. Ma X, Zhang T, Luo Z, Li X, Lin M, Li R, et al. Functional nanovector boost anti-atherosclerosis efficacy of berberine in ApoE^{-/-} mice. *Acta Pharm Sin B* 2020;**10**:1769–83.
 40. Szmítko PE, Wang CH, Weisel RD, de Almeida JR, Anderson TJ, Verma S. New markers of inflammation and endothelial cell activation: part I. *Circulation* 2003;**108**:1917–23.
 41. Qi Q, Hu WJ, Zheng SL, Zhang SL, Le YY, Li ZY, et al. Metrnl deficiency decreases blood HDL cholesterol and increases blood triglyceride. *Acta Pharmacol Sin* 2020;**41**:1568–75.
 42. El-Ashmawy HM, Selim FO, Hosny TAM, Almassry HN. Association of low serum Meteorin like (Metrnl) concentrations with worsening of glucose tolerance, impaired endothelial function and atherosclerosis. *Diabetes Res Clin Pract* 2019;**150**:57–63.
 43. Liu ZX, Ji HH, Yao MP, Wang L, Wang Y, Zhou P, et al. Serum Metrnl is associated with the presence and severity of coronary artery disease. *J Cell Mol Med* 2019;**23**:271–80.
 44. Miao ZW, Hu WJ, Li ZY, Miao CY. Involvement of the secreted protein Metrnl in human diseases. *Acta Pharmacol Sin* 2020;**41**:1525–30.
 45. Libby P. The changing landscape of atherosclerosis. *Nature* 2021;**592**:524–33.
 46. Teng C, Lin C, Huang F, Xing X, Chen S, Ye L, et al. Intracellular codelivery of anti-inflammatory drug and anti-miR 155 to treat inflammatory disease. *Acta Pharm Sin B* 2020;**10**:1521–33.
 47. Tian L, Lu L, Feng J, Melancon MP. Radiopaque nano and polymeric materials for atherosclerosis imaging, embolization and other catheterization procedures. *Acta Pharm Sin B* 2018;**8**:360–70.
 48. Jung TW, Pyun DH, Kim TJ, Lee HJ, Park ES, Abd El-Aty AM, et al. Meteorin-like protein (METRNL)/IL-41 improves LPS-induced inflammatory responses via AMPK or PPARdelta-mediated signaling pathways. *Adv Med Sci* 2021;**66**:155–61.
 49. Gao X, Leung TF, Wong GW, Ko WH, Cai M, He EJ, et al. Meteorin-beta/Meteorin like/IL-41 attenuates airway inflammation in house dust mite-induced allergic asthma. *Cell Mol Immunol* 2022;**19**:245–59.
 50. Zuo L, Ge S, Ge Y, Li J, Zhu B, Zhang Z, et al. The adipokine Metrnl ameliorates chronic colitis in *Il-10*^{-/-} mice by attenuating mesenteric adipose tissue lesions during spontaneous colitis. *J Crohns Colitis* 2019;**13**:931–41.
 51. Yao Z, Lin P, Wang C, Wang K, Sun Y. Administration of metrnl delays the onset of diabetes in non-obese diabetic mice. *Endocr J* 2021;**68**:179–88.
 52. Hu W, Wang R, Sun B. Meteorin-like ameliorates beta cell function by inhibiting beta cell apoptosis of and promoting beta cell proliferation via activating the WNT/beta-catenin pathway. *Front Pharmacol* 2021;**12**:627147.